



Journal of Advances in Modeling Earth Systems (JAMES)

Supporting Information for

Addressing Challenges in Simulating Inter-annual Variability of Gross Primary Production

Ranit De^{1,2}✉, Shanning Bao^{1,3}, Sujan Koirala¹, Alexander Brenning^{2,4}, Markus Reichstein^{1,4}, Torben Tagesson⁵, Michael Liddell⁶, Andreas Ibrom⁷, Sebastian Wolf⁸, Ladislav Šigut⁹, Lukas Hörtnagl⁸, William Woodgate^{10,11}, Mika Korkiakoski¹², Lutz Merbold¹³, T. Andrew Black¹⁴, Marilyn Roland¹⁵, Anne Klosterhalfen¹⁶, Peter D. Blanken¹⁷, Sara Knox^{18,19}, Simone Sabbatini²⁰, Bert Gielen¹⁵, Leonardo Montagnani²¹, Rasmus Fensholt²², Georg Wohlfahrt²³, Ankur R. Desai²⁴, Eugénie Paul-Limoges²⁵, Marta Galvagno²⁶, Albin Hammerle²³, Georg Jocher^{27,9}, Borja Ruiz Reverte²⁸, David Holl²⁹, Jiquan Chen³⁰, Luca Vitale³¹, M. Altaf Arain³², and Nuno Carvalhais^{1,4,33}✉

¹Department for Biogeochemical Integration, Max Planck Institute for Biogeochemistry, 07745, Jena, Germany

²Friedrich Schiller University Jena, Department of Geography, Löbdergraben 32, 07743, Jena, Germany

³National Space Science Center, Chinese Academy of Sciences, 100190, Beijing, China

⁴ELLIS Unit Jena, Jena, Germany

⁵Department of Physical Geography and Ecosystem Science, Lund University, Sölvegatan 12, SE-223 62 Lund, Sweden

⁶Centre for Tropical, Environmental, and Sustainability Sciences, James Cook University, Cairns, Queensland, Australia

⁷Department of Environment and Resource Engineering, Technical University of Denmark (DTU), Bygningstorvet 115, 2800 Kgs. Lyngby, Denmark

⁸Department of Environmental Systems Science, ETH Zürich, 8092, Zürich, Switzerland

⁹Global Change Research Institute of the Czech Academy of Sciences, Belidla 4a, 60300, Brno, Czech Republic

¹⁰School of the Environment, The University of Queensland, St Lucia 4072, Australia

¹¹CSIRO, Space and Astronomy, Kensington, 6151, WA, Australia

¹²Finnish Meteorological Institute, Climate System Research Unit, P.O. Box 503, 00101 Helsinki, Finland

¹³Integrative Agroecology Group, Agroscope, 8046, Zürich, Switzerland

¹⁴Faculty of Land and Food Systems, University of British Columbia, Vancouver, British Columbia V6T 1Z4, Canada

¹⁵Plants and Ecosystems (PLECO), Department of Biology, University of Antwerp, B-2610 Wilrijk, Belgium

¹⁶Bioclimatology, University of Goettingen, 37077, Goettingen, Germany

¹⁷Department of Geography, University of Colorado Boulder, Boulder, CO 80309, USA

¹⁸Department of Geography, McGill University, Montreal, Quebec H3A 0B9, Canada

¹⁹Department of Geography, The University of British Columbia, Vancouver, British Columbia V6T 1Z2, Canada

²⁰CMCC Foundation - Euro-Mediterranean Center on Climate Change, 73100, Lecce, Italy

²¹Faculty of Agricultural, Environmental and Food Sciences, Free University of Bozen-Bolzano, 39100, Bolzano, Italy

²²Department of Geosciences and Natural Resource Management, University of Copenhagen, Øster Voldgade 10, DK-1350 Copenhagen, Denmark

²³Universität Innsbruck, Institut für Ökologie, Sternwartestr. 15, 6020 Innsbruck, Austria

²⁴Dept of Atmospheric and Oceanic Sciences, University of Wisconsin-Madison, Madison, WI 53706 USA

²⁵Swiss Federal Institute for Forest, Snow and Landscape Research (WSL), 8903, Birmensdorf, Switzerland

²⁶Environmental Protection Agency of Aosta Valley, Climate Change Unit, (ARPA Valle d'Aosta), 11020, Saint-Christophe AO, Italy

²⁷Thünen Institute of Climate-Smart Agriculture, Bundesallee 65, 38116, Braunschweig, Germany

²⁸Departamento de Química e Física, Universidade Federal da Paraíba - Campus II, 58397-000 Areia, Paraíba, Brazil

²⁹University Hamburg, Institute of Soil Science, 20146, Hamburg, Germany

³⁰Department of Geography, Environment, and Spatial Sciences, Michigan State University, MI 48823, USA

³¹Institute for Agriculture and Forestry Systems in the Mediterranean (ISAFoM), P.le Enrico Fermi 1, 80055, Portici, Italy

³²School of Earth, Environment and Society, McMaster University, Hamilton, Ontario L8S 4K1, Canada

³³CENSE, Departamento de Ciências e Engenharia do Ambiente, Faculdade de Ciências e Tecnologia, Universidade NOVA de Lisboa, Caparica, Portugal

Contents of this file

1. [Text S1 to Text S5](#)
2. [Figures S1 to S10](#)
3. [Tables S1 to S8](#)

Introduction

This supporting information file contains details on the calculation of the water availability indicator ([Text S1](#), Fig. [S1](#)), additional details on P-model description and equations ([Text S2](#), Fig. [S2](#), Table [S1](#)), a short discussion on some of the supporting results ([Text S3 – Text S5](#)), figure to support the choice of a model equation (Fig. [S3](#)), a figure showing the location of sites used in the study (Fig. [S4](#)), figures (Fig. [S5 – S10](#)) and tables (Tables [S2 – S7](#)) to supplement the results presented in the main text, and details on site characteristics (Table [S8](#)).

✉ Corresponding author: Ranit De, rde@bgc-jena.mpg.de or de.ranit19@gmail.com

✉ Corresponding author: Nuno Carvalhais, ncarvalhais@bgc-jena.mpg.de

Text S1 Calculation of Water Availability Indicator (WAI)

WAI was calculated using a water bucket model, similar to the methods of Bao et al. (2022), as a proxy for the soil moisture available to the vegetation (Tramontana et al., 2016). This model (Fig. S1) is a simplified version of the hydrological model used in the study of Trautmann et al. (2018).

Text S2 Implementation of Drought Stress in the P_{hr}^W Model

We implemented a drought stress function to improve hourly gross primary production (GPP) estimates produced by the P_{hr} model. We calculated hourly instantaneous GPP with the instantaneous values of forcing data following the equations in Fig. S2. Then the acclimated GPP (GPP_{acclim_t}) was calculated at each timestep t by considering acclimation (on the parameters shown with sky blue box in Fig. S2) as described in Sect. 2.2 of Mengoli et al. (2022).

We calculated *WAI* using the method described in Text S1. Then we calculated a drought stress function (Bao et al., 2022; Horn & Schulz, 2011) as shown in Eq. (S1) and (S2). W_t in Eq. (S2) denotes soil water supply, i.e., WAI_t/AWC at timestep t , as described in Table 1 of the main paper. The symbols in bold are calibrated parameters as described in Table 1 of the main paper. The lag parameter (α) for soil moisture effect was only parameterized for arid sites where the Köppen–Geiger (KG) climate class starts with ‘B’ (Beck et al., 2018; Rubel et al., 2017).

$$fW_t = \frac{1}{1 + \exp(\mathbf{k}_W(W_{f_t} - W_I))} \quad (\text{S1})$$

$$W_{f_t} = (1 - \alpha) \cdot W_t + \alpha \cdot W_{f_{t-1}} \quad (\text{S2})$$

To calculate our final hourly simulated GPP (GPP_{sim_t}) by the P_{hr}^W model, we multiplied the GPP_{acclim_t} produced by P_{hr} model at each timestep t , with corresponding values of fW_t , viz. Eq. (S3).

$$GPP_{sim_t} = GPP_{acclim_t} \times fW_t \quad (\text{S3})$$

Text S3 Performance of P_{hr}^W , P_{hr} Models in an Irrigated C₄ Cropland

The P_{hr}^W model failed to capture the annual average of GPP fluxes in an irrigated cropland for most of the years (Fig. S6). This could be due to an inaccurate estimation of drought stress as we do not consider any information on irrigation. Moreover, this site is a C₄ cropland, and no distinct treatments were formulated in the P_{hr}^W model for C₄ vegetation.

Text S4 Bao_{dd} Model Performance: Site-specific Example

The Bao_{dd} model was originally parameterized using daily data by Bao et al. (2022). We wanted to perform a direct comparison in model performance between the Bao_{hr} model and the Bao_{dd} model. Bao_{dd} model captured the annual average of eddy covariance derived GPP better in the case of site-year and site-specific model parameterization compared to the two other generalized parameterization strategies, i.e., PFT-specific and global parameterization (Fig. S7).

Text S5 Model Performance at Different Climate–vegetation Types

The median model performance decreases from site–year-specific to site-specific to PFT-specific to global parameterization for most climate–vegetation types and both P_{hr}^W and Bao_{hr} models (Fig. S9). At temperate grasslands and boreal forests, the median values of NNSE are similar per PFT and global parameterization of the P_{hr}^W model. At boreal forests, the median values of NNSE are similar per PFT and global parameterization of the Bao_{hr} model as well.

For the parameterization of the P_{hr}^W model, the highest median value of NNSE was found for tropical forests and tropical grasslands for per-site–year parameterization (median NNSE: 0.89), tropical forests for per-site parameterization (median NNSE: 0.88), tropical grasslands for per-PFT parameterization (median NNSE: 0.80), and temperate forests for global parameterization (median NNSE: 0.76). For Bao_{hr} model parameterization experiments, the highest median value of NNSE was found for tropical forests for per-site–year (median NNSE: 0.91), per-site (median

NNSE: 0.9), and global (median NNSE: 0.8) parameterization experiments, and tropical grasslands for per-PFT (median NNSE: 0.81) parameterization experiments.

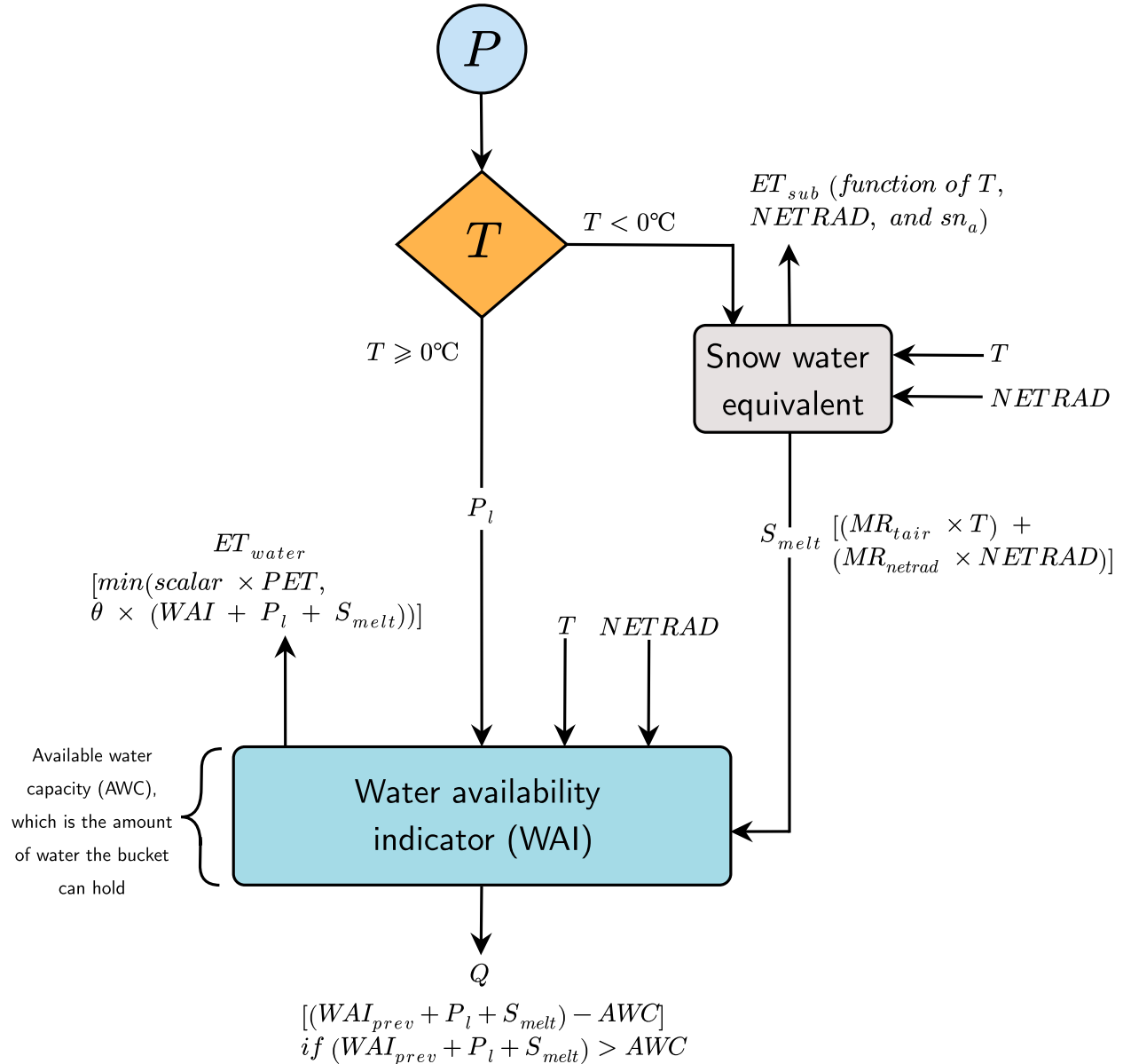


Figure S1: The schematic of the water bucket model used in this study. P , T , PET , and $NETRAD$ are precipitation, temperature, potential evapotranspiration, and net radiation respectively, and were used as forcing (see Table A1 of the main paper). P_l , ET_{sub} , ET_{water} , S_{melt} , and Q are liquid precipitation, evapotranspiration by sublimation, evapotranspiration from the water bucket, water melted from snow, and runoff respectively. Simulated evapotranspiration (ET_{sim}), which was used in the cost function was calculated as the sum of ET_{water} and ET_{sub} . θ , AWC , PET_{scalar} , sn_a , MR_{tair} , and MR_{netrad} are the calibrated model parameters. The description of these parameters can be found in Table 1 of the main paper.

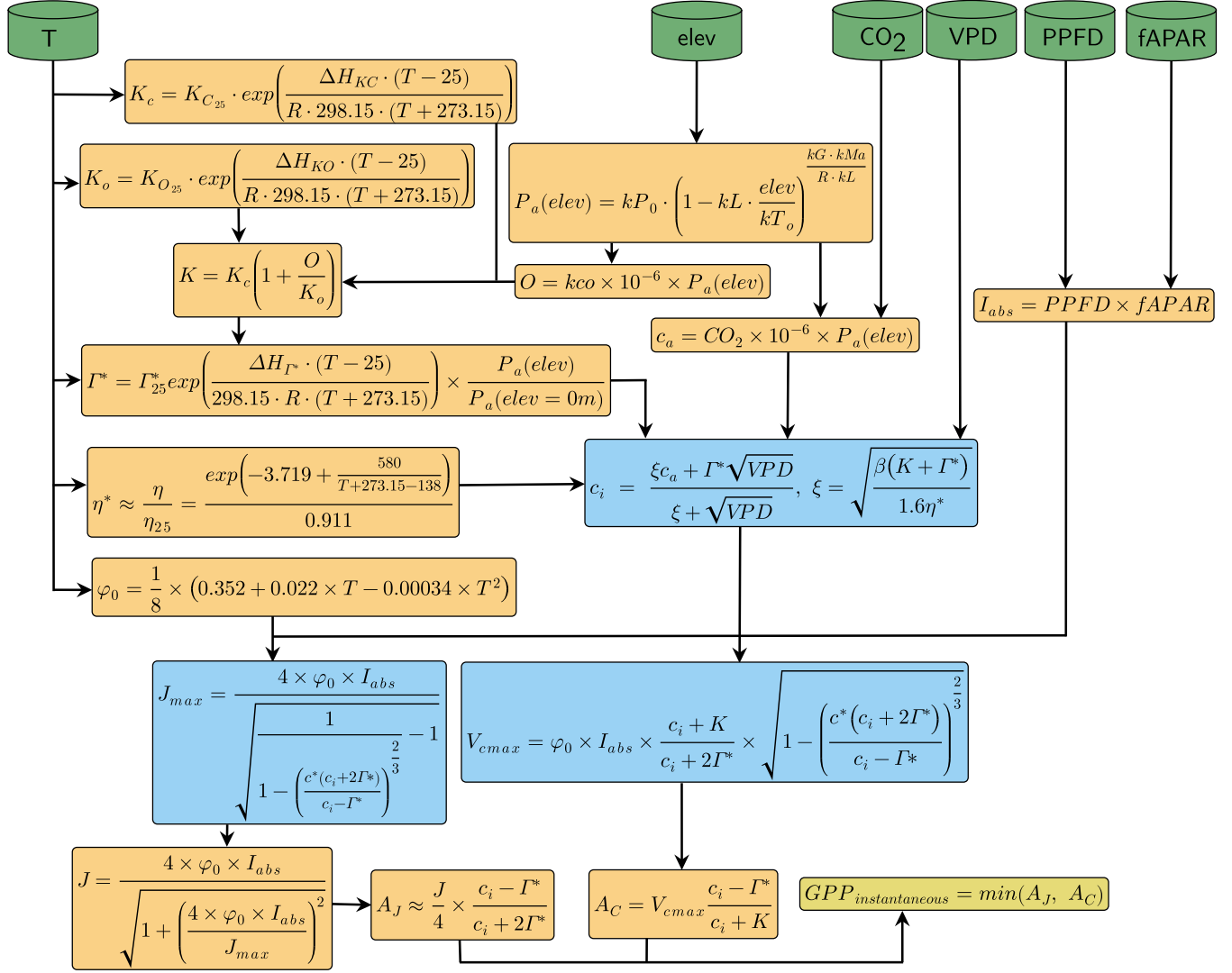


Figure S2: A slightly revised version of the P_{hr} model schematics. This figure is adapted from Fig. 1 of Mengoli et al. (2022). The variables in dark green are forcing data as described in Table A1 of the main paper. The model parameters in this figure are described in Table S1. The parameters in the sky blue box are the parameters considered for acclimation. The box with an olive green color shows the model output.

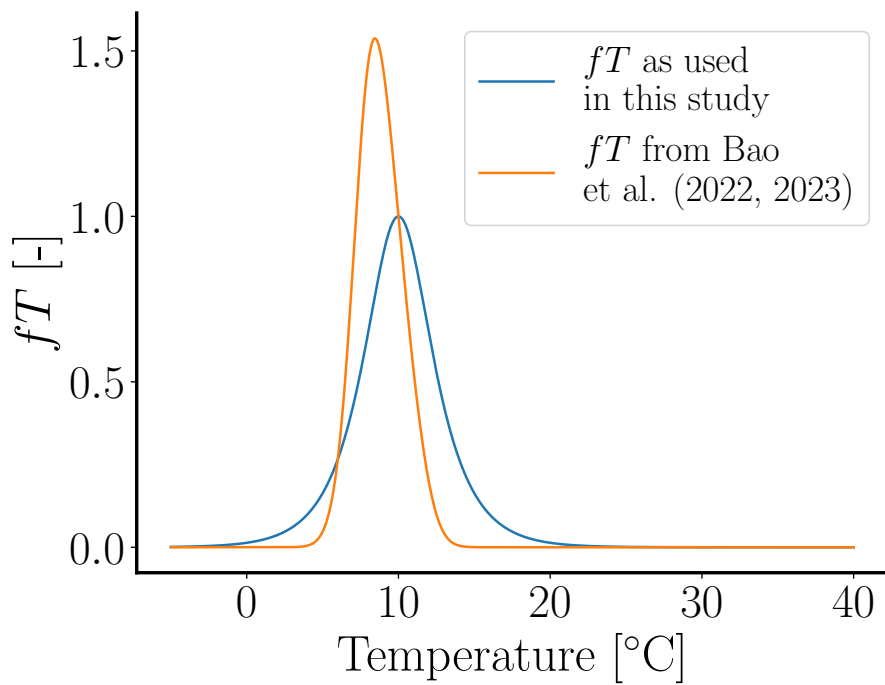


Figure S3: Comparison of partial sensitivity function of temperature (fT) between Bao et al. (2022, 2023) and a slightly modified version which was used in this study. The modified version produced values of fT between zero and one for a typical temperature range. Whereas, the previous version can produce values of fT greater than one for optimal temperature.

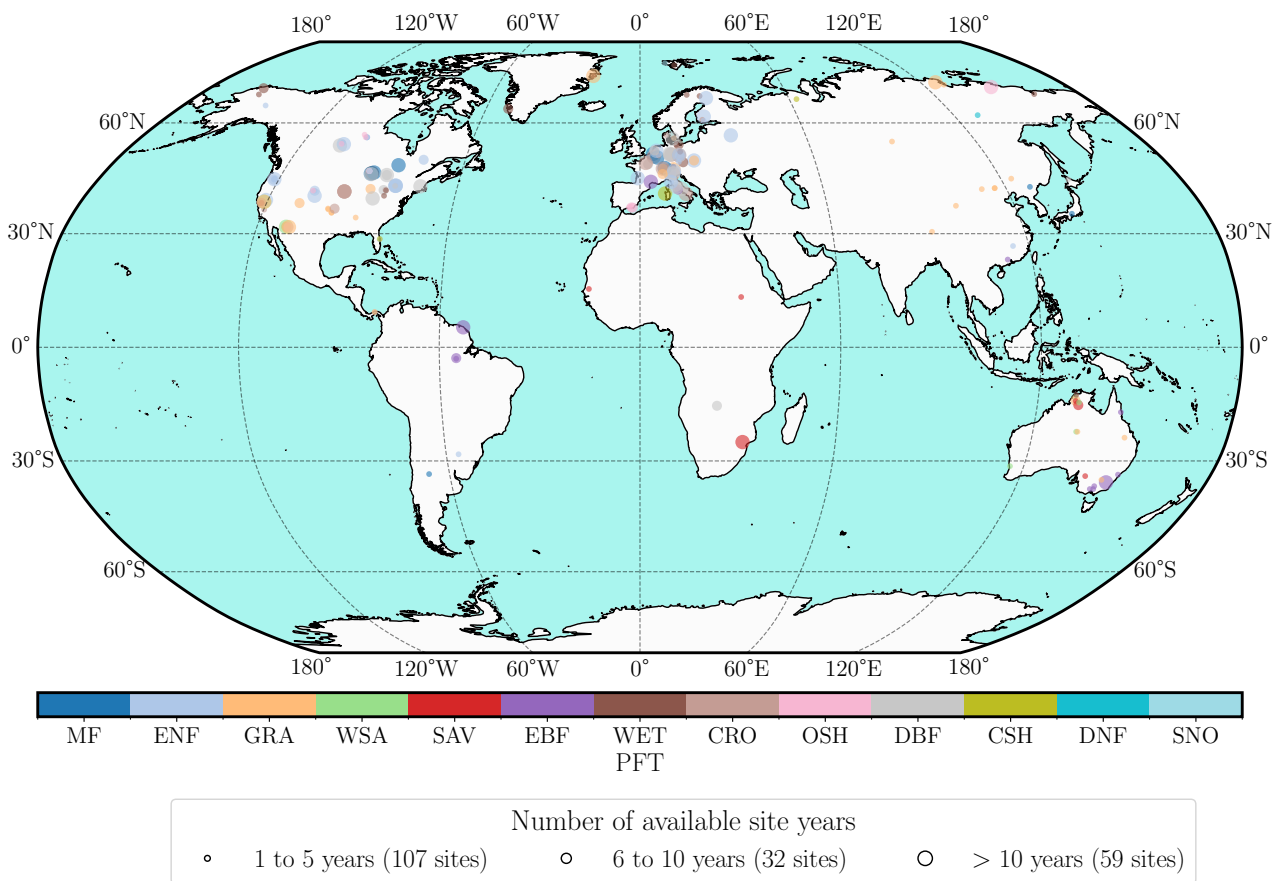


Figure S4: The distribution of a total of 198 EC sites used in this study. The sites represent a wide variety of plant-functional types (PFT), located in varying latitudinal sections, and contain measurement records of varying lengths. The description of PFTs can be found in FLUXNET.org (2024). The coastlines and islands were provided by Elson et al. (2023).

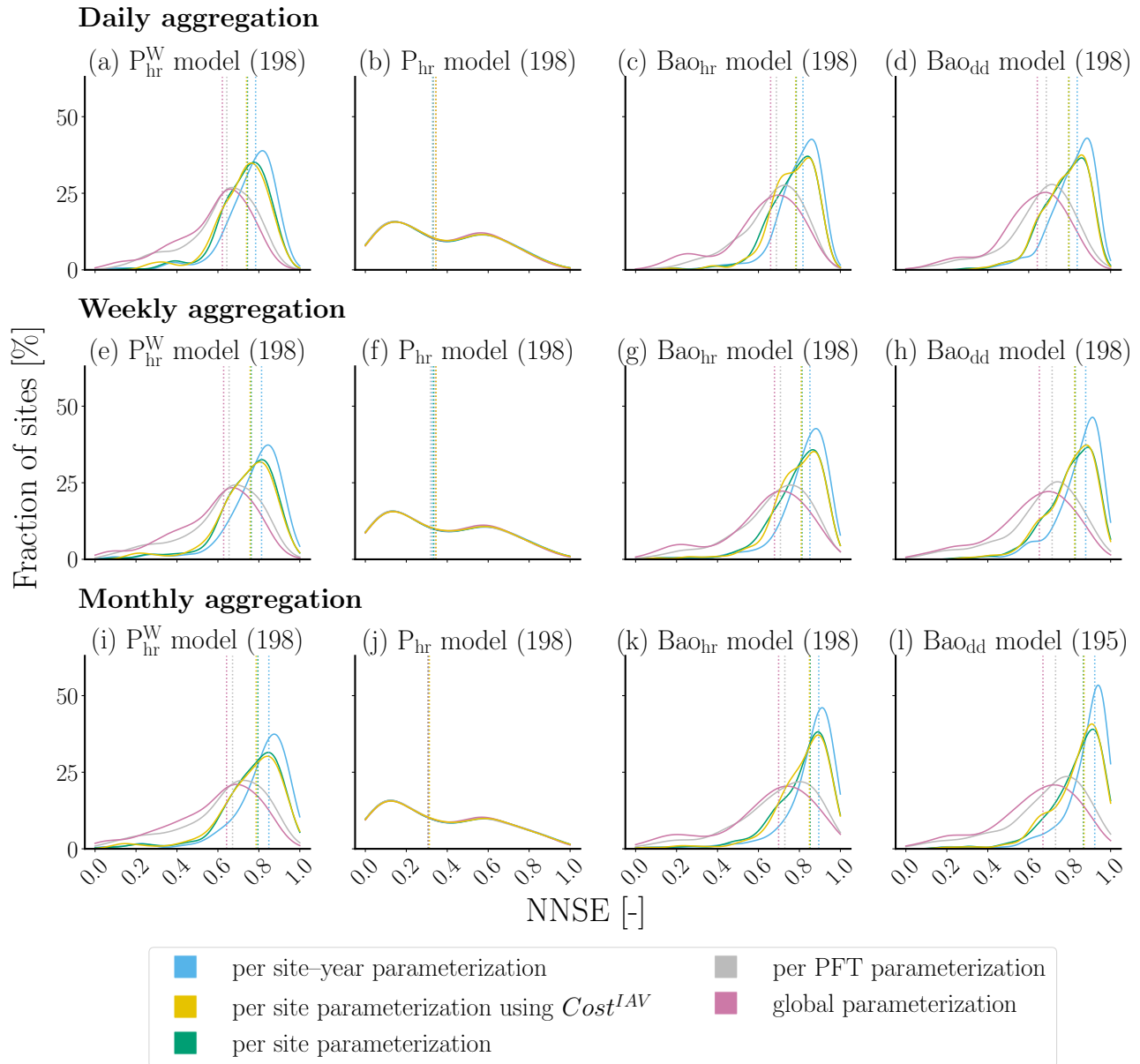


Figure S5: Distributions of model performance measure (normalized Nash-Sutcliffe efficiency, viz. NNSE) at daily scale (first row), at weekly scale (second row), and at monthly scale (third row) from P-model of Mengoli et al. (2022) with drought stress parameterized at hourly scale (P_{hr}^W), P-model of Mengoli et al. (2022) without drought stress parameterized at hourly scale (P_{hr}), global best model of Bao et al. (2022) parameterized at hourly scale (Bao_{hr}), and global best model of Bao et al. (2022) parameterized at daily scale (Bao_{dd}). The dotted vertical lines represent the median model performance, which are summarized in Table S2. The numbers in parentheses beside the model name on top of each of the sub-figures represent the total number of sites. The model performance at a monthly scale could be calculated for fewer sites as some sites have a very low measurement period (see Appendix C of the main paper).

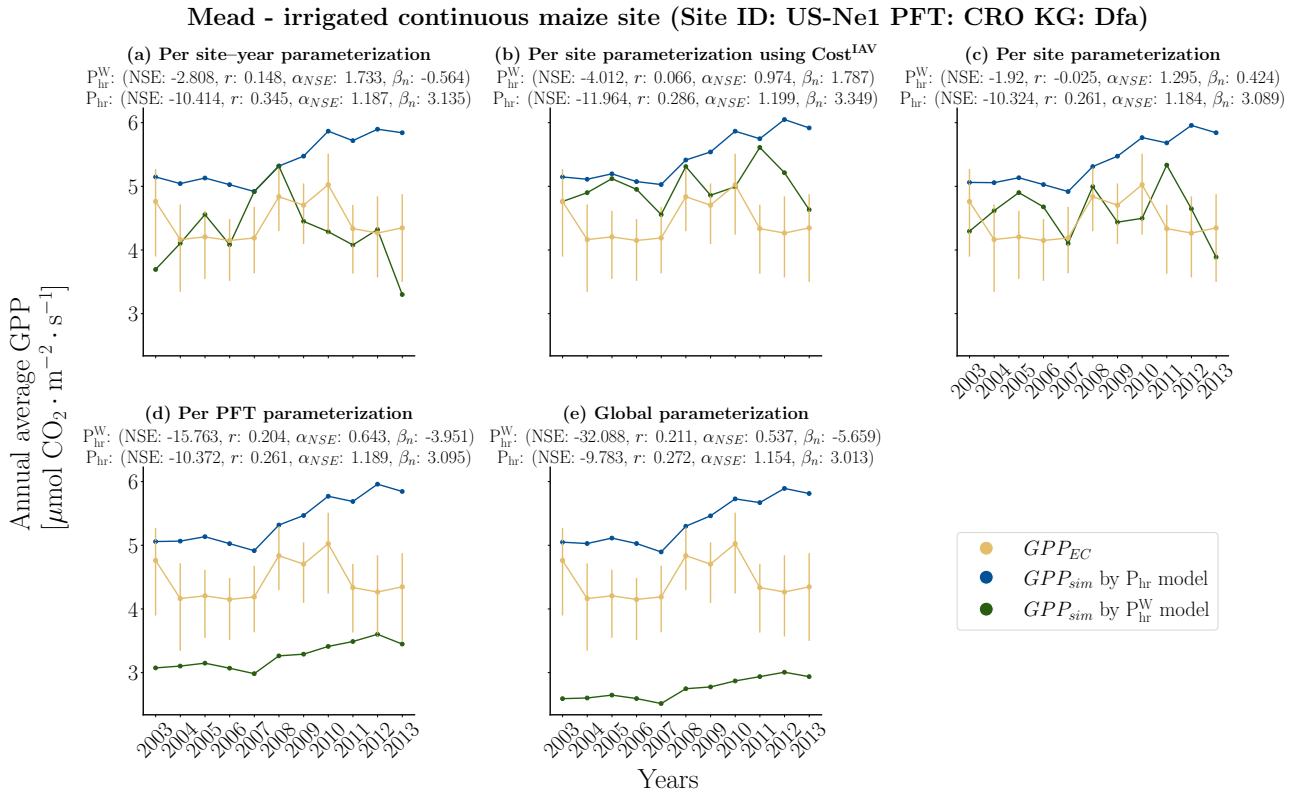


Figure S6: Comparison of annual average of gross primary production (GPP) derived by eddy covariance measurements (GPP_{EC}), and GPP simulated (GPP_{sim}) by the P-model of Mengoli et al. (2022) parameterized at hourly scale without drought stress (P_{hr} model) and with drought stress (P_{hr}^W model). The five subplots show simulated GPP from **(a)** site–year specific parameterization, **(b)** site-specific parameterization using an additional constraint on inter-annual variability in the cost function ($Cost^{IAV}$), **(c)** site-specific parameterization, **(d)** plant-functional types (PFT) specific parameterization, and **(e)** global parameterization. The values of the model performance measure (Nash-Sutcliffe efficiency, viz. NSE, correlation coefficient, viz. r , relative variability, viz. α_{NSE} , and bias, viz. β_n) are shown on top of respective subplots. Maize is cultivated in this site and has an annual average temperature of $\approx 10.55^\circ\text{C}$, and an annual average precipitation of ≈ 832.2 mm during the observation period (Pastorello et al., 2020; Suyker, 2016a). The vertical error bars represent the uncertainty range (see Sect. 2.4.3 of the main paper) of the annual average of GPP_{EC} for the corresponding years. The site ID, PFT, and Köppen–Geiger climate class (KG) of the site are provided on top of the figure in bold.

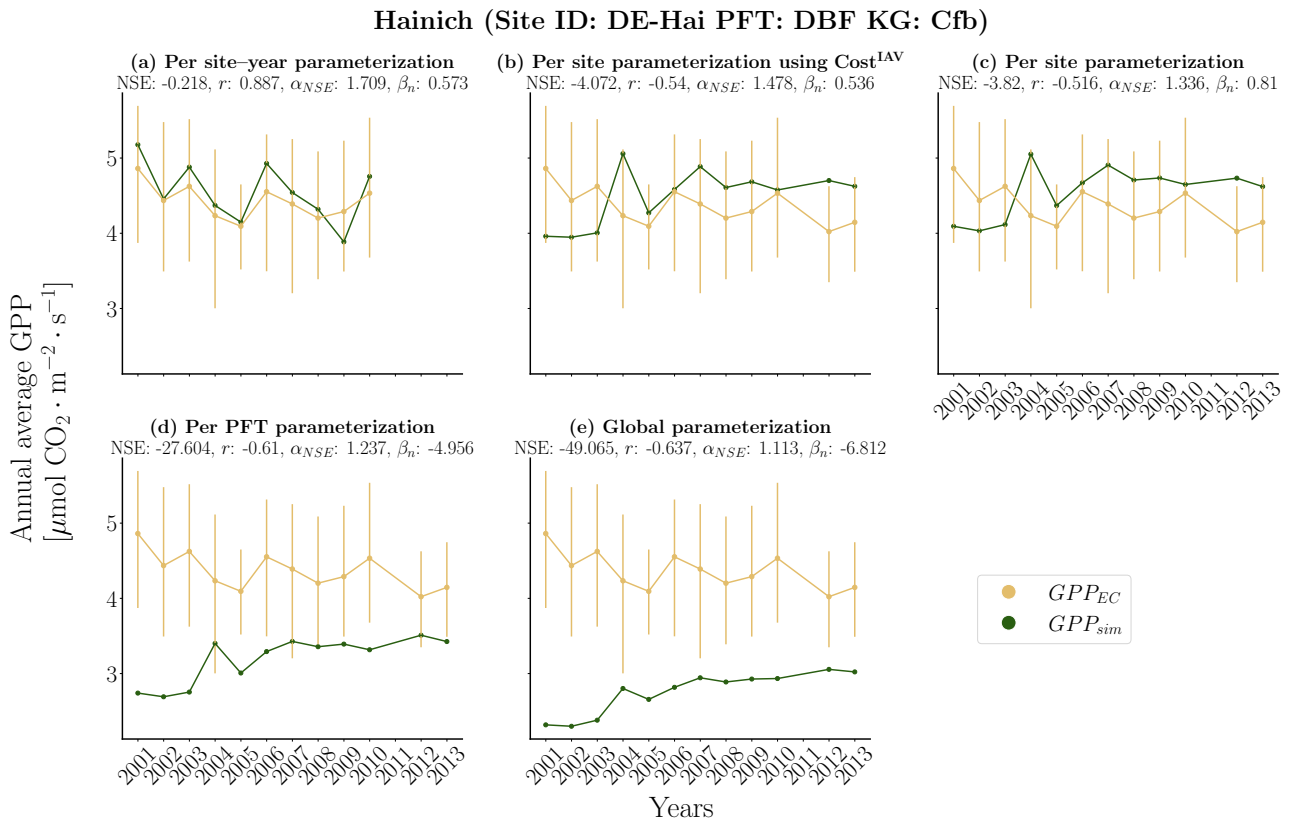


Figure S7: Comparison of annual average of gross primary production (GPP) derived by eddy covariance measurements (GPP_{EC}), and GPP simulated (GPP_{sim}) by the light use efficiency model of Bao et al. (2022), which was parameterized with daily data (Bao_{dd} model). The five subplots show simulated GPP from **(a)** site–year specific parameterization, **(b)** site-specific parameterization using an additional constraint on inter-annual variability in the cost function ($Cost^{IAV}$), **(c)** site-specific parameterization, **(d)** plant-functional types (PFT) specific parameterization, and **(e)** global parameterization. The years 2010 to 2012 could not be parameterized in the case of site–year parameterization, as there were no good quality evapotranspiration estimates from latent heat flux measurements for those years. The values of the model performance measure (Nash-Sutcliffe efficiency, viz. NSE, correlation coefficient, viz. r , relative variability, viz. α_{NSE} , and bias, viz. β_n) are shown on top of respective subplots. This site represents an average 140-year-old deciduous forest (Tamrakar et al., 2018) with a distinct seasonal cycle and an annual average temperature of ≈ 8.3 °C, and an annual average precipitation of 750–800 mm during the observation period (Knohl et al., 2003a; Pastorello et al., 2020). The vertical error bars represent the uncertainty range (see Sect. 2.4.3 of the main paper) of the annual average of GPP_{EC} for the corresponding years. The site ID, PFT, and Köppen–Geiger climate class (KG) of the site are provided on top of the figure in bold.

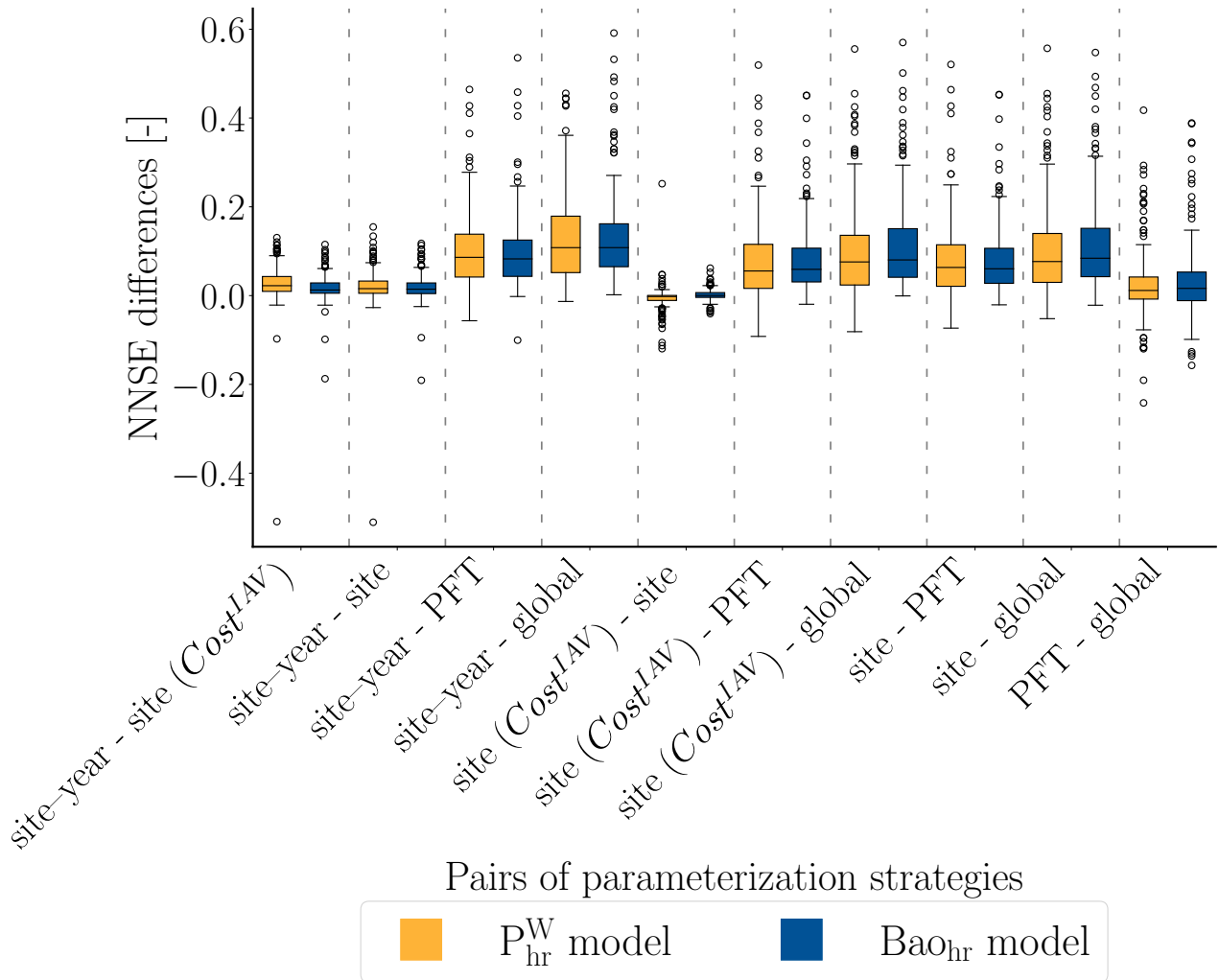


Figure S8: Distributions of the differences between model performance measures (normalized Nash-Sutcliffe efficiency, viz. NNSE) calculated at hourly scale, from various pairs of model parameterization experiments conducted for the P-model of Mengoli et al. (2022) with drought stress, parameterized with hourly data (P^W_{hr} model) and the light use efficiency model of Bao et al. (2022), parameterized with hourly data (Bao_{hr} model). Cost_{IAV} in parentheses denotes the usage of an additional constraint on annual gross primary production flux during per-site parameterization. The boxes are spanned between the first and third quartiles of the differences, and the line in the middle represents the median. The whiskers show the farthest data point from the box within $1.5 \times$ of the interquartile range. The circles represent the outliers that go beyond the limits of the whiskers. The vertical dotted grey lines separate each pair of model parameterization strategies.

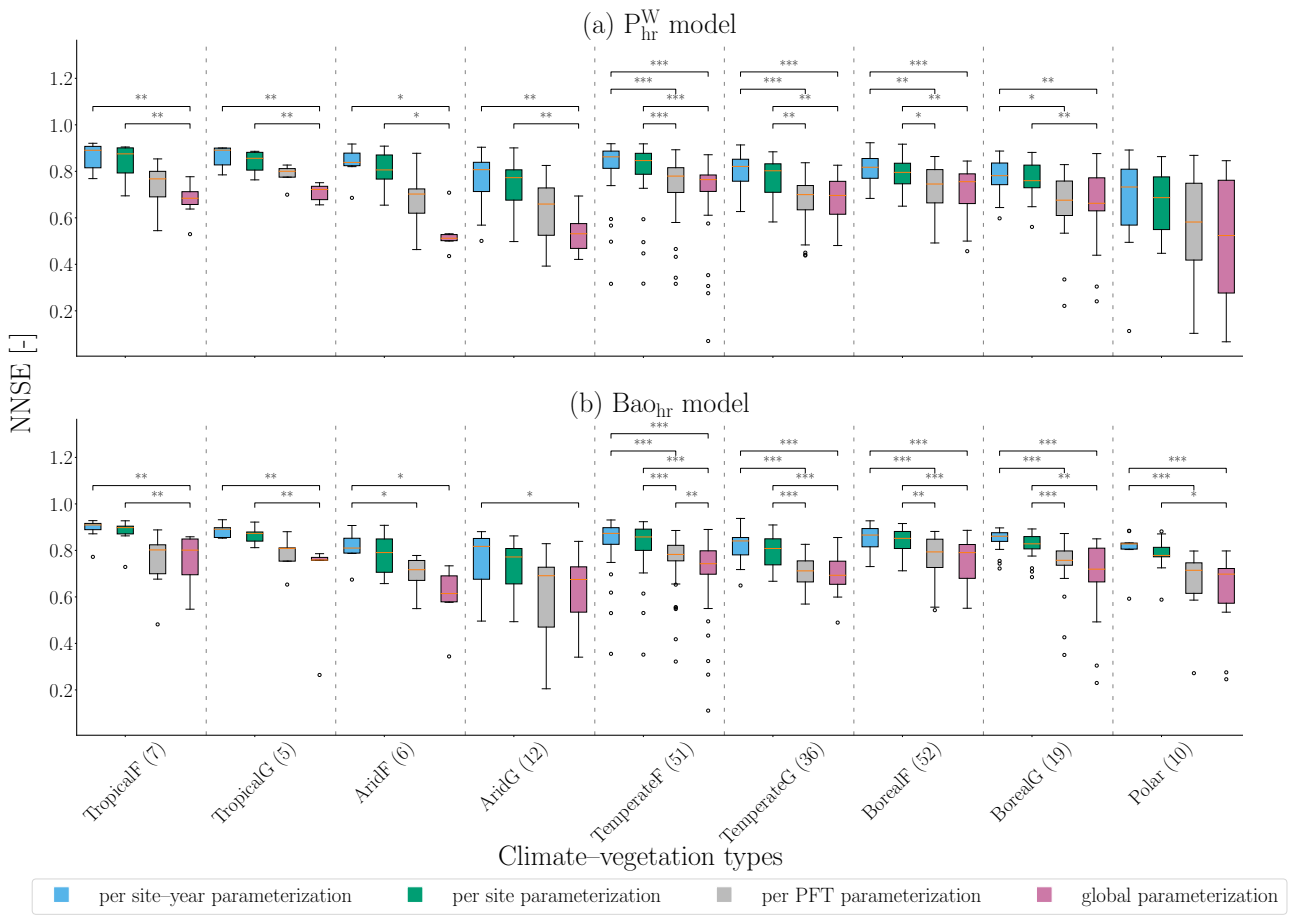


Figure S9: Box-plots showing the range of the hourly model performance metric (normalized Nash-Sutcliffe efficiency, viz. NNSE) for the sites in different climate–vegetation types, and different parameterization experiments. The subplots show the model performance for the **(a)** P_{hr}^W model of Mengoli et al. (2022) with drought stress function, parameterized with hourly data (P_{hr}^W model), and **(b)** the light use efficiency model of Bao et al. (2022) parameterized with hourly data (Bao_{hr} model). The numbers in parenthesis beside the name of each climate–vegetation type on the x-axis are the number of sites present in a specific climate–vegetation type. The boxes are spanned between the first and third quartiles of NNSE values, and the line in the middle represents the median. The whiskers show the farthest data point from the box which is within 1.5× of the inter-quartile range. The circles represent the outliers that go beyond the limits of the whiskers. The results of statistical significance testing using a two-sample Kolmogorov-Smirnov test (Hodges, 1958) between a pair of model parameterization strategies (connecting bars over boxplots) are shown as * (0.05 > p-value ≥ 0.01), ** (0.01 > p-value ≥ 0.001), *** (p-value < 0.001) if the distributions of model performances were not identical. No bars and star symbols over a pair of boxplots signify that the distributions of model performances from a pair of parameterization strategies were identical and the null hypothesis could not be rejected (p-value ≥ 0.05). The vertical dotted grey lines separate each climate–vegetation type.

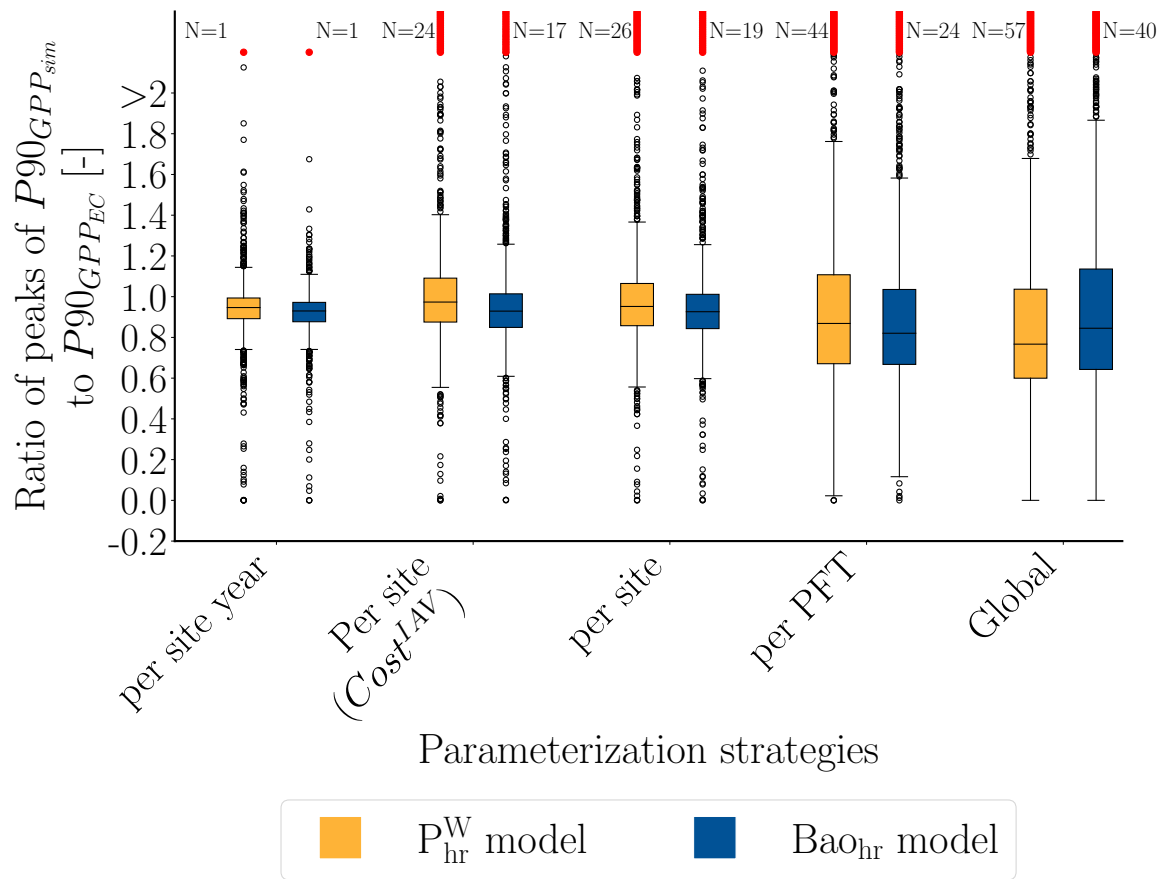


Figure S10: Distributions of the ratios of percentile 90 of simulated gross primary production ($P90_{GPP_{sim}}$) to percentile 90 of gross primary production derived from eddy covariance measurements ($P90_{GPP_{EC}}$). The $P90_{GPP_{sim}}$ was estimated from the gross primary production simulated (GPP_{sim}) by the P-model of Mengoli et al. (2022) with drought stress function which was parameterized with hourly data (P^W_{hr} model), and the light use efficiency model of Bao et al. (2022) which was also parameterized with hourly data (Bao_{hr} model). The boxes are spanned between the first and third quartiles of the ratios, and the line in the middle represents the median. The whiskers show the farthest data point from the box within $1.5 \times$ of the interquartile range. The white circles represent the outliers that go beyond the limits of the whiskers (but ≤ 2.2). The solid dark red circles are the outliers that go beyond 2.2. N represents the total number of such sites for the respective distribution.

Table S1: Description of the P_{hr} model parameters. After Mengoli et al. (2022).

Symbol	Description	Value and/or unit	Reference
$V_{c_{max}}$	Maximum rate of carboxylation (or maximum rate of Rubisco activity)	$\mu\text{molCO}_2 \cdot \text{m}^{-2} \cdot \text{s}^{-1}$	Mengoli et al. (2022)
ΔH_a	Activation energy for $V_{c_{max}}$	$65330 \text{ J} \cdot \text{mol}^{-1}$	Mengoli et al. (2022)
J_{max}	Maximum rate of electron transport	$\mu\text{mol electrons} \cdot \text{m}^{-2} \cdot \text{s}^{-1}$	Mengoli et al. (2022)
$\Delta H_{a,j}$	Activation energy for J_{max}	$43900 \text{ J} \cdot \text{mol}^{-1}$	Mengoli et al. (2022)
R	Universal gas constant	$8.314 \text{ J} \cdot \text{mol}^{-1} \cdot \text{K}^{-1}$	Mengoli et al. (2022)
$\chi = c_i : c_a$	Ratio of leaf-internal to ambient partial pressures of CO_2	-	Mengoli et al. (2022)
c_i	Leaf-internal CO_2 partial pressure	Pa	Mengoli et al. (2022)
c_a	Ambient CO_2 partial pressure	Pa	Mengoli et al. (2022)
ξ	Sensitivity of χ to vapor pressure deficit	$\text{Pa}^{0.5}$	Mengoli et al. (2022)
$\varphi_0(T)$	Temperature dependence function of quantum efficiency	$\text{mol} \cdot \text{mol}^{-1}$	Mengoli et al. (2022)
β	The ratio of cost factors for carboxylation and transpiration capacities at 25°C	146 [-]	Mengoli et al. (2022)
c^*	The cost factor for electron-transport capacity	0.41 [-]	Mengoli et al. (2022)
K_c	Michaelis–Menten constant for carboxylation	Pa	Mengoli et al. (2022)
$K_{C_{25}}$	Michaelis–Menten constant for carboxylation at 25°C	39.97 Pa	Mengoli et al. (2022)
ΔH_{KC}	Activation energy for K_c	$79430 \text{ J} \cdot \text{mol}^{-1}$	Mengoli et al. (2022)
K_O	Michaelis–Menten constant for oxygenation	Pa	Mengoli et al. (2022)
$K_{O_{25}}$	Michaelis–Menten constant for oxygenation at 25°C	27480 Pa	Mengoli et al. (2022)
ΔH_{KO}	Activation energy for K_O	$36380 \text{ J} \cdot \text{mol}^{-1}$	Mengoli et al. (2022)
K	The effective Michaelis–Menten coefficient for Rubisco kinetics	Pa	Mengoli et al. (2022)
kP_o	Standard atmospheric pressure at 0 m a.s.l.	101325 Pa	Stocker et al. (2020)
kL	Mean adiabatic lapse rate	$0.0065 \text{ K} \cdot \text{m}^{-2}$	Stocker et al. (2020)
kT_o	Base temperature	298.15 K	Stocker and Hufkens (2021)
kG	Gravitational constant	$9.80665 \text{ m} \cdot \text{s}^{-2}$	Stocker et al. (2020)
kM_a	Molecular weight for dry air	$0.028963 \text{ kg} \cdot \text{mol}^{-1}$	Stocker et al. (2020)
kco	Partial pressure of oxygen with kP_o	$2.09476 \times 10^5 \text{ Pa}$	Stocker et al. (2020)
Γ^*	Photorespiratory compensation point	Pa	Mengoli et al. (2022)
Γ_{25}^*	Photorespiratory compensation point at 25°C	4.332 Pa	Mengoli et al. (2022)
ΔH_{Γ^*}	Activation energy for Γ^*	$37830 \text{ J} \cdot \text{mol}^{-1}$	Mengoli et al. (2022)
η^*	Temperature dependence of the viscosity of the water, relative to its value at 25°C	-	Mengoli et al. (2022)
$P_a(\text{elev})$	Atmospheric pressure at given elevation a.s.l (elev)	Pa	Mengoli et al. (2022)
J	Rate of electron transport	$\mu\text{mol electrons} \cdot \text{m}^{-2} \cdot \text{s}^{-1}$	Mengoli et al. (2022)
A_C	Rubisco-limited assimilation rate	$\mu\text{molCO}_2 \cdot \text{m}^{-2} \cdot \text{s}^{-1}$	Mengoli et al. (2022)
A_J	Electron-transport limited assimilation rate	$\mu\text{molCO}_2 \cdot \text{m}^{-2} \cdot \text{s}^{-1}$	Mengoli et al. (2022)
A	Assimilation rate	$\mu\text{molCO}_2 \cdot \text{m}^{-2} \cdot \text{s}^{-1}$	Mengoli et al. (2022)

Table S2: Median normalized Nash-Sutcliffe efficiency (NNSE) obtained at each modelling experiment at daily, weekly, and monthly aggregations

Temporal resolution	Models	Parameterization strategies				
		Per site-year	Per site using <i>Cost^{IAV}</i>	Per site	Per PFT	Global
Daily aggregation/ scale	P ^W _{hr}	0.784	0.740	0.744	0.643	0.622
	P _{hr}	0.329	0.344	0.331	0.331	0.345
	Bao _{hr}	0.817	0.782	0.784	0.688	0.659
	Bao _{dd}	0.837	0.796	0.796	0.686	0.642
Weekly aggregation	P ^W _{hr}	0.813	0.758	0.762	0.654	0.628
	P _{hr}	0.326	0.346	0.334	0.318	0.343
	Bao _{hr}	0.851	0.809	0.813	0.707	0.678
	Bao _{dd}	0.878	0.824	0.827	0.714	0.652
Monthly aggregation	P ^W _{hr}	0.849	0.787	0.795	0.672	0.642
	P _{hr}	0.307	0.313	0.309	0.305	0.308
	Bao _{hr}	0.895	0.849	0.853	0.729	0.698
	Bao _{dd}	0.922	0.870	0.867	0.731	0.670

Table S3: Sum of squared error (SSE) values obtained from modeling experiments of various complexities

Temporal scale/ aggregation	Models	Parameterization strategies				
		Per site-year	Per site	Per site	Per PFT	Global
using Cost^{IAV}						
Hourly scale	P _{hr} ^W	7.41×10 ⁷	8.60×10 ⁷	8.84×10 ⁷	1.31×10 ⁸	1.49×10 ⁸
Daily scale/	Bao _{hr}	6.10 × 10 ⁷	7.13 × 10 ⁷	7.01 × 10 ⁷	1.22 × 10 ⁸	1.32 × 10 ⁸
Monthly aggregation	P _{hr} ^W	1.20×10 ⁶	1.45×10 ⁶	1.48×10 ⁶	2.45×10 ⁶	2.84×10 ⁶
Yearly aggregation	Bao _{hr}	9.59 × 10 ⁵	1.16 × 10 ⁶	1.15 × 10 ⁶	2.29 × 10 ⁶	2.47 × 10 ⁶
Hourly scale	Bao _{dd}	6.19 × 10 ⁵	8.30 × 10 ⁵	8.51 × 10 ⁵	1.65 × 10 ⁶	2.04 × 10 ⁶
Daily scale/	P _{hr} ^W	2.49×10 ⁴	3.26×10 ⁴	3.25×10 ⁴	6.41×10 ⁴	7.75×10 ⁴
Monthly aggregation	Bao _{hr}	1.72 × 10 ⁴	2.27 × 10 ⁴	2.28 × 10 ⁴	5.94 × 10 ⁴	6.41 × 10 ⁴
Yearly aggregation	Bao _{dd}	1.01 × 10 ⁴	1.70 × 10 ⁴	1.76 × 10 ⁴	4.39 × 10 ⁴	5.68 × 10 ⁴
Hourly scale	P _{hr} ^W	2.61×10 ²	5.11×10 ²	3.64×10 ²	1.88×10 ³	2.48×10 ³
Daily scale/	Bao _{hr}	3.44 × 10 ²	3.67 × 10 ²	4.14 × 10 ²	2.21 × 10 ³	2.43 × 10 ³
Monthly aggregation	Bao _{dd}	1.04 × 10 ²	2.34 × 10 ²	2.51 × 10 ²	1.48 × 10 ³	1.97 × 10 ³

Table S4: Sample size (*n*) used in of various modeling experiments

Temporal scale/ aggregation	Models	Parameterization strategies				
		Per site-year	Per site	Per site	Per PFT	Global
using Cost^{IAV}						
Hourly scale	P _{hr} ^W	7.51×10 ⁶	7.54×10 ⁶	7.54×10 ⁶	7.54×10 ⁶	7.54×10 ⁶
Daily scale/	Bao _{hr}	7.51×10 ⁶	7.54×10 ⁶	7.54×10 ⁶	7.54×10 ⁶	7.54×10 ⁶
Monthly aggregation	P _{hr} ^W	3.57×10 ⁵	3.58×10 ⁵	3.58×10 ⁵	3.58×10 ⁵	3.58×10 ⁵
Yearly aggregation	Bao _{hr}	3.57×10 ⁵	3.58×10 ⁵	3.58×10 ⁵	3.58×10 ⁵	3.58×10 ⁵
Hourly scale	Bao _{dd}	2.81×10 ⁵	2.81×10 ⁵	2.81×10 ⁵	2.81×10 ⁵	2.81×10 ⁵
Daily scale/	P _{hr} ^W	1.21×10 ⁴	1.21×10 ⁴	1.21×10 ⁴	1.21×10 ⁴	1.21×10 ⁴
Monthly aggregation	Bao _{hr}	1.21×10 ⁴	1.21×10 ⁴	1.21×10 ⁴	1.21×10 ⁴	1.21×10 ⁴
Yearly aggregation	Bao _{dd}	9.87×10 ³	9.89×10 ³	9.89×10 ³	9.89×10 ³	9.89×10 ³
Hourly scale	P _{hr} ^W	1.01×10 ³	1.01×10 ³	1.01×10 ³	1.01×10 ³	1.01×10 ³
Daily scale/	Bao _{hr}	1.01×10 ³	1.01×10 ³	1.01×10 ³	1.01×10 ³	1.01×10 ³
Monthly aggregation	Bao _{dd}	8.70×10 ²	8.72×10 ²	8.72×10 ²	8.72×10 ²	8.72×10 ²

Table S5: Total number of parameters (K) parameterized in modeling experiments of various complexities. The number of parameters only varies between parameterization strategies as more parameters were parameterized for finer parameterization strategies and are the same across all the temporal scale/ aggregations.

Models	Parameterization strategies				
	Per site-year	Per site	Per site	Per PFT	Global
using Cost^{IAV}					
P _{hr} ^W	1.18×10 ⁴	1.83×10 ³	1.83×10 ³	1.23×10 ²	1.00×10 ¹
Bao _{hr}	2.34×10 ⁴	3.60×10 ³	3.60×10 ³	2.39×10 ²	1.90×10 ¹
Bao _{dd}	2.33×10 ⁴	3.60×10 ³	3.60×10 ³	2.39×10 ²	1.90×10 ¹

Table S6: P-values obtained by performing two-sample Kolmogorov-Smirnov test (Hodges, 1958) between samples of performances for a plant-functional type (PFT) from P-model of Mengoli et al. (2022) with drought stress function, parameterized with hourly data (P_{hr}^W model) and the light use efficiency model of Bao et al. (2022) parameterized with hourly data (Bao_{hr} model) for a specific parameterization strategy. The symbols beside the p-values signify if the distribution of model performance were identical or not: *n.s.* (p-value ≥ 0.05 , distributions were identical and null hypothesis could not be rejected), * ($0.05 > \text{p-value} \geq 0.01$, distributions were not identical and null hypothesis was rejected), ** ($0.01 > \text{p-value} \geq 0.001$, distributions were not identical and null hypothesis was rejected), * * * ($\text{p-value} < 0.001$, distributions were not identical and null hypothesis was rejected)

PFT	Parameterization strategies			
	Per site-year	Per site	Per PFT	Global
CRO	0.306 <i>n.s.</i>	0.027*	0.068 <i>n.s.</i>	0.068 <i>n.s.</i>
CSH	1.0 <i>n.s.</i>	1.0 <i>n.s.</i>	0.6 <i>n.s.</i>	0.6 <i>n.s.</i>
DBF	0.006**	0.006**	0.71 <i>n.s.</i>	0.156 <i>n.s.</i>
DNF	1.0 <i>n.s.</i>	1.0 <i>n.s.</i>	1.0 <i>n.s.</i>	1.0 <i>n.s.</i>
EBF	0.588 <i>n.s.</i>	0.999 <i>n.s.</i>	0.588 <i>n.s.</i>	0.588 <i>n.s.</i>
ENF	0.153 <i>n.s.</i>	0.054 <i>n.s.</i>	0.03*	0.03*
GRA	0.69 <i>n.s.</i>	0.492 <i>n.s.</i>	0.199 <i>n.s.</i>	0.492 <i>n.s.</i>
MF	0.352 <i>n.s.</i>	0.126 <i>n.s.</i>	0.352 <i>n.s.</i>	0.352 <i>n.s.</i>
OSH	0.3 <i>n.s.</i>	0.898 <i>n.s.</i>	0.126 <i>n.s.</i>	0.3 <i>n.s.</i>
SAV	0.931 <i>n.s.</i>	0.931 <i>n.s.</i>	0.931 <i>n.s.</i>	0.143 <i>n.s.</i>
SNO	1.0 <i>n.s.</i>	1.0 <i>n.s.</i>	1.0 <i>n.s.</i>	1.0 <i>n.s.</i>
WET	0.004**	0.081 <i>n.s.</i>	0.336 <i>n.s.</i>	0.571 <i>n.s.</i>
WSA	0.931 <i>n.s.</i>	0.931 <i>n.s.</i>	0.931 <i>n.s.</i>	0.931 <i>n.s.</i>

Table S7: P-values obtained by performing two-sample Kolmogorov-Smirnov test (Hodges, 1958) between samples of performances for a climate–vegetation type from P-model of Mengoli et al. (2022) with drought stress function, parameterized with hourly data (P_{hr}^W model) and the light use efficiency model of Bao et al. (2022) parameterized with hourly data (Bao_{hr} model) for a specific parameterization strategy. The symbols beside the p-values signify if the distribution of model performance were identical or not: n.s. (p-value ≥ 0.05 , distributions were identical and null hypothesis could not be rejected), * ($0.05 > \text{p-value} \geq 0.01$, distributions were not identical and null hypothesis was rejected), ** ($0.01 > \text{p-value} \geq 0.001$, distributions were not identical and null hypothesis was rejected), *** ($\text{p-value} < 0.001$, distributions were not identical and null hypothesis was rejected)

Climate–vegetation type	Parameterization strategies			
	Per site–year	Per site	Per PFT	Global
TropicalF	0.575 ^{n.s.}	0.963 ^{n.s.}	0.963 ^{n.s.}	0.053 ^{n.s.}
TropicalG	0.873 ^{n.s.}	0.873 ^{n.s.}	1.0 ^{n.s.}	0.079 ^{n.s.}
AridF	0.931 ^{n.s.}	0.931 ^{n.s.}	0.931 ^{n.s.}	0.143 ^{n.s.}
AridG	0.998 ^{n.s.}	0.998 ^{n.s.}	0.869 ^{n.s.}	0.1 ^{n.s.}
TemperateF	0.408 ^{n.s.}	0.562 ^{n.s.}	0.877 ^{n.s.}	0.283 ^{n.s.}
TemperateG	0.707 ^{n.s.}	0.51 ^{n.s.}	0.51 ^{n.s.}	0.34 ^{n.s.}
BorealF	0.004 ^{**}	0.002 ^{**}	0.077 ^{n.s.}	0.046 [*]
BorealG	0.009 ^{**}	0.027 [*]	0.068 ^{n.s.}	0.306 ^{n.s.}
Polar	0.052 ^{n.s.}	0.168 ^{n.s.}	0.418 ^{n.s.}	0.787 ^{n.s.}

Table S8: Details of 198 EC sites used in this study. Site ID is the ID of a site assigned by Pastorello et al. (2020). Lat, Lon, Obs. period, PFT, KG, Elev. are latitude, longitude, observation period, plant function type, Köppen–Geiger climate class, and elevation (in m). Site PFT and KG are the same as assigned by Pastorello et al. (2020), and elevations were taken from Table S2 of Bao et al. (2022). We assign PFT of the site AU-ASM as WSA (contrary to SAV as assigned by Pastorello et al., 2020) as this site represents woody Mulga (*Acacia aneura*) and seasonal grassy surface layer (Cleverly, Boulain, Villalobos-Vega, et al., 2013).

Site ID	Lat	Lon	Obs. period	PFT	KG	Elev.	Reference
AR-SLu	-33.46	-66.46	2009 to 2011	MF	BSh	506.0	Garcia et al. (2016) and Ulke et al. (2015)
AR-Vir	-28.24	-56.19	2010 to 2012	ENF	Cfa	105.0	Posse et al. (2016a) and Posse et al. (2016b)
AT-Neu	47.12	11.32	2002 to 2012	GRA	Dfc	970.0	Wohlfahrt et al. (2008, 2016)
AU-Ade	-13.08	131.12	2007 to 2009	WSA	Aw	90.0	Beringer, Hacker, et al. (2011) and Beringer and Hutley (2016a)
AU-ASM	-22.28	133.25	2010 to 2014	WSA	BWh	606.0	Cleverly, Boulain, Villalobos-Vega, et al. (2013) and Cleverly and Eamus (2016a)
AU-Cpr	-34.0	140.59	2010 to 2014	SAV	BSk	62.0	W. S. Meyer et al. (2015) and W. Meyer et al. (2016)
AU-Cum	-33.61	150.72	2012 to 2014	EBF	Cfa	20.0	Beringer, Hutley, et al. (2016) and Pendall and Griebel (2016)

Continued on next page

Table S8 – *Continued from previous page*

Site ID	Lat	Lon	Obs. period	PFT	KG	Elev.	Reference
AU-DaP	-14.06	131.32	2007 to 2013	GRA	Aw	71.0	Beringer and Hutley (2016b) and Beringer, Hutley, et al. (2011)
AU-DaS	-14.16	131.39	2008 to 2011	SAV	Aw	110.0	Beringer and Hutley (2016c) and Hutley et al. (2011)
AU-Dry	-15.26	132.37	2008 to 2014	SAV	Aw	175.0	Beringer and Hutley (2016d) and Cernusak et al. (2011)
AU-Emr	-23.86	148.47	2011 to 2013	GRA	BSh	170.0	Schroder (2014) and Schroder et al. (2016)
AU-Fog	-12.55	131.31	2006 to 2008	WET	Aw	4.0	Beringer and Hutley (2016e) and Beringer et al. (2013)
AU-Gin	-31.38	115.71	2011 to 2013	WSA	Csa	51.0	Macfarlane et al. (2016)
AU-RDF	-14.56	132.48	2011 to 2013	WSA	Aw	188.0	Beringer and Hutley (2016f) and Bristow et al. (2016)
AU-Rob	-17.12	145.63	2014	EBF	Cfa	710.0	Beringer, Hutley, et al. (2016) and Liddell (2016)
AU-TTE	-22.29	133.64	2012 to 2014	GRA	BWh	553.0	Cleverly and Eamus (2016b)
AU-Tum	-35.66	148.15	2001 to 2014	EBF	Cfb	1200.0	Leuning et al. (2005) and Woodgate et al. (2016)

Continued on next page

Table S8 – *Continued from previous page*

Site ID	Lat	Lon	Obs. period	PFT	KG	Elev.	Reference
AU-Wac	-37.43	145.19	2005 to 2008	EBF	Cfb	545.0	Beringer, Hutley, et al. (2016) and Kilinc et al. (2013)
AU-Whr	-36.67	145.03	2011 to 2014	EBF	Cfa	165.0	Beringer, Cunningham, et al. (2016) and McHugh et al. (2017)
AU-Wom	-37.42	144.09	2010 to 2014	EBF	Cfb	705.0	Arndt et al. (2016)
AU-Ync	-34.99	146.29	2012 to 2014	GRA	BSk	126.0	Beringer and Walker (2016) and Yee et al. (2015)
BE-Bra	51.31	4.52	1999 to 2014	MF	Cfb	16.0	Carrara et al. (2004) and Neirynck et al. (2016)
BE-Lon	50.55	4.75	2004 to 2014	CRO	Cfb	167.0	De Ligne, Manise, Moureaux, et al. (2016) and Moureaux et al. (2006)
BE-Vie	50.31	6.0	1996 to 2014	MF	Cfb	450.0	Aubinet et al. (2001) and De Ligne, Manise, Heinesch, et al. (2016)
BR-Sa1	-2.86	-54.96	2002 to 2011	EBF	Am	88.0	T. R. Baker et al. (2004) and Saleska (2016)
BR-Sa3	-3.02	-54.97	2000 to 2004	EBF	Am	100.0	Asner et al. (2004) and Goulden (2016a)
CA-Gro	48.22	-82.16	2003 to 2014	MF	Dfb	340.0	A. Barr et al. (2013) and McCaughey (2016)

Continued on next page

Table S8 – *Continued from previous page*

Site ID	Lat	Lon	Obs. period	PFT	KG	Elev.	Reference
CA-NS2	55.91	-98.52	2001 to 2005	ENF	Dfc	260.0	D. Baldocchi and Penuelas (2019) and Goulden (2016b)
CA-NS3	55.91	-98.38	2001 to 2005	ENF	Dfc	260.0	D. Baldocchi and Penuelas (2019) and Goulden (2016c)
CA-NS4	55.91	-98.38	2002 to 2005	ENF	Dfc	260.0	D. Baldocchi and Penuelas (2019) and Goulden (2016d)
CA-NS5	55.86	-98.48	2001 to 2005	ENF	Dfc	260.0	D. Baldocchi and Penuelas (2019) and Goulden (2016e)
CA-NS6	55.92	-98.96	2001 to 2005	OSH	Dfc	244.0	D. Baldocchi and Penuelas (2019) and Goulden (2016f)
CA-NS7	56.64	-99.95	2002 to 2005	OSH	Dfc	297.0	D. Baldocchi and Penuelas (2019) and Goulden (2016g)
CA-Oas	53.63	-106.2	1996 to 2010	DBF	Dfc	530.0	A. G. Barr et al. (2004) and Black (2016a)
CA-Obs	53.99	-105.12	1999 to 2010	ENF	Dfc	628.94	A. Barr et al. (2013) and Black (2016b)
CA-Qfo	49.69	-74.34	2003 to 2010	ENF	Dfc	382.0	D. Baldocchi and Penuelas (2019) and Margolis (2016)
CA-SF1	54.48	-105.82	2003 to 2006	ENF	Dfc	536.0	Amiro (2009, 2016a)
CA-SF2	54.25	-105.88	2001 to 2005	ENF	Dfc	520.0	Amiro (2009, 2016b)
CA-SF3	54.09	-106.01	2002 to 2006	OSH	Dfc	540.0	Amiro (2009, 2016c)

Continued on next page

Table S8 – *Continued from previous page*

Site ID	Lat	Lon	Obs. period	PFT	KG	Elev.	Reference
CA-TP1	42.66	-80.56	2003 to 2014	ENF	Dfb	265.0	Arain (2016a) and Arain and Restrepo-Coupe (2005)
CA-TP2	42.77	-80.46	2003 to 2007	ENF	Dfb	212.0	Arain (2016b) and Arain and Restrepo-Coupe (2005)
CA-TP3	42.71	-80.35	2003 to 2014	ENF	Dfb	184.0	Arain (2016c) and Arain and Restrepo-Coupe (2005)
CA-TP4	42.71	-80.36	2002 to 2014	ENF	Dfb	184.0	Arain (2016d) and Arain and Restrepo-Coupe (2005)
CA-TPD	42.64	-80.56	2012 to 2014	DBF	Dfb	260.0	Arain (2016e) and Chu et al. (2018)
CH-Cha	47.21	8.41	2005 to 2014	GRA	Cfb	393.0	Hörtnagl, Feigenwinter, et al. (2016a) and Merbold et al. (2014)
CH-Dav	46.82	9.86	1997 to 2014	ENF	ET	1639.0	Hörtnagl, Eugster, Merbold, et al. (2016) and Zielis et al. (2014)
CH-Fru	47.12	8.54	2005 to 2014	GRA	Cfb	982.0	Hörtnagl, Feigenwinter, et al. (2016b) and Imer et al. (2013)
CH-Lae	47.48	8.36	2004 to 2014	MF	Cfb	689.0	Etzold et al. (2011) and Hörtnagl, Eugster, Buchmann, et al. (2016)

Continued on next page

Table S8 – *Continued from previous page*

Site ID	Lat	Lon	Obs. period	PFT	KG	Elev.	Reference
CH-Oe1	47.29	7.73	2002 to 2008	GRA	Cfb	450.0	Ammann et al. (2009) and Ammann (2016)
CH-Oe2	47.29	7.73	2004 to 2014	CRO	Cfb	452.0	Dietiker et al. (2010) and Hörtnagl, Maier, et al. (2016)
CN-Cha	42.4	128.1	2003 to 2005	MF	Dwb	738.0	Guan et al. (2006) and Zhang and Han (2016)
CN-Cng	44.59	123.51	2007 to 2010	GRA	BSk	171.0	Dong (2016)
CN-Dan	30.5	91.07	2004 to 2005	GRA	Dwc	4286.0	Shi et al. (2006, 2016)
CN-Din	23.17	112.54	2003 to 2005	EBF	Cfa	507.0	Yu et al. (2006) and Zhou and Yan (2016)
CN-Du2	42.05	116.28	2007 to 2008	GRA	Dwb	1350.0	S. Chen (2016) and S. Chen et al. (2009)
CN-Du3	42.06	116.28	2009 to 2010	GRA	Dwb	1350.0	Shao (2016a)
CN-HaM	37.37	101.18	2002 to 2004	GRA	ET	3190.0	Kato et al. (2006) and Tang et al. (2016)
CN-Qia	26.74	115.06	2003 to 2005	ENF	Cfa	109.0	Wang and Fu (2016) and Yu et al. (2006)
CN-Sw2	41.79	111.9	2010 to 2012	GRA	BSk	1438.0	Shao (2016b)
CZ-BK1	49.5	18.54	2004 to 2014	ENF	Dfb	908.0	Acosta et al. (2013) and Sigut et al. (2016a)
CZ-BK2	49.49	18.54	2006 to 2012	GRA	Dfb	855.0	Sigut et al. (2016b)
CZ-wet	49.02	14.77	2006 to 2014	WET	Cfb	426.0	Dušek et al. (2012) and Dušek et al. (2016)
DE-Akm	53.87	13.68	2009 to 2014	WET	Cfb	-1.0	Bernhofer et al. (2016a)

Continued on next page

Table S8 – *Continued from previous page*

Site ID	Lat	Lon	Obs. period	PFT	KG	Elev.	Reference
DE-Geb	51.1	10.91	2001 to 2014	CRO	Cfb	161.5	P. M. Anthoni et al. (2004) and Brümmer et al. (2016)
DE-Gri	50.95	13.51	2004 to 2014	GRA	Cfb	385.0	Bernhofer et al. (2016b) and Prescher et al. (2010)
DE-Hai	51.08	10.45	2000 to 2012	DBF	Cfb	430.0	Knohl, Tiedemann, Kolle, Schulze, Kutsch, et al. (2016) and Knohl et al. (2003b)
DE-Kli	50.89	13.52	2004 to 2014	CRO	Cfb	478.0	Bernhofer et al. (2016c) and Prescher et al. (2010)
DE-Lkb	49.1	13.3	2009 to 2013	ENF	Dfb	1308.0	Lindauer et al. (2014) and Lindauer et al. (2016)
DE-Lnf	51.33	10.37	2002 to 2012	DBF	Cfb	451.0	P. M. Anthoni et al. (2004) and Knohl, Tiedemann, Kolle, Schulze, Anthoni, et al. (2016)
DE-Obe	50.78	13.72	2008 to 2014	ENF	Cfb	734.0	Bernhofer et al. (2016d)
DE-Seh	50.87	6.45	2007 to 2010	CRO	Cfb	103.0	Schmidt et al. (2012) and Schneider and Schmidt (2016)
DE-SfN	47.81	11.33	2012 to 2014	WET	Cfb	590.0	Hommeltenberg et al. (2014) and Klatt et al. (2016)

Continued on next page

Table S8 – *Continued from previous page*

Site ID	Lat	Lon	Obs. period	PFT	KG	Elev.	Reference
DE-Spw	51.89	14.03	2010 to 2014	WET	Cfb	61.0	Bernhofer et al. (2016e)
DE-Tha	50.96	13.57	1996 to 2014	ENF	Cfb	380.0	Bernhofer et al. (2016f) and Grünwald and Bernhofer (2007)
DE-Zrk	53.88	12.89	2013 to 2014	WET	Cfb	0.0	Sachs et al. (2016) and Zak et al. (2015)
DK-Eng	55.69	12.19	2005 to 2008	GRA	Cfb	10.0	Pilegaard and Ibrom (2016)
DK-Fou	56.48	9.59	2005	CRO	Cfb	51.0	Olesen (2016)
DK-Sor	55.49	11.64	1996 to 2014	DBF	Cfb	40.0	Ibrom and Pilegaard (2016) and Pilegaard et al. (2011)
ES-Amo	36.83	-2.25	2007 to 2012	OSH	BSh	58.0	López-Ballesteros et al. (2017) and Poveda et al. (2016)
ES-LgS	37.1	-2.97	2007 to 2009	OSH	Csb	2267.0	Reverter et al. (2010) and Reverter et al. (2016a)
ES-LJu	36.93	-2.75	2004 to 2013	OSH	Csa	1600.0	Cañete et al. (2016) and Serrano-Ortiz et al. (2009)
ES-Ln2	36.97	-3.48	2009	OSH	Csb	2249.0	Reverter et al. (2016b)
FI-Hyy	61.85	24.3	1996 to 2014	ENF	Dfc	181.0	Mammarella et al. (2016) and Suni et al. (2003)

Continued on next page

Table S8 – *Continued from previous page*

Site ID	Lat	Lon	Obs. period	PFT	KG	Elev.	Reference
FI-Jok	60.9	23.51	2000 to 2003	CRO	Dfb	109.0	Lohila, Aurela, Tuovinen, et al. (2016) and Lohila et al. (2004)
FI-Let	60.64	23.96	2009 to 2012	ENF	Dfb	111.0	Korkiakoski et al. (2017) and Lohila, Korkiakoski, et al. (2016)
FI-Lom	68.0	24.21	2007 to 2009	WET	Dfc	269.0	Aurela, Lohila, Tuovinen, Hatakka, et al. (2016) and Aurela et al. (2015)
FI-Sod	67.36	26.64	2001 to 2014	ENF	Dfc	180.0	Aurela, Tuovinen, et al. (2016) and Thum et al. (2007)
FR-Fon	48.48	2.78	2005 to 2014	DBF	Cfb	92.0	Bazot et al. (2013) and Berveiller et al. (2016)
FR-Gri	48.84	1.95	2004 to 2014	CRO	Cfb	125.0	Buyssse et al. (2016) and Loubet et al. (2011)
FR-LBr	44.72	-0.77	1996 to 2008	ENF	Cfb	61.0	Berbigier and Lous- tau (2016) and Berbigier et al. (2001)
FR-Pue	43.74	3.6	2000 to 2014	EBF	Csa	270.0	Ourcival (2016) and Rambal et al. (2004)
GF-Guy	5.28	-52.92	2004 to 2014	EBF	Am	48.0	Bonal and Burban (2016) and Bonal et al. (2008)

Continued on next page

Table S8 – *Continued from previous page*

Site ID	Lat	Lon	Obs. period	PFT	KG	Elev.	Reference
GL-NuF	64.13	-51.39	2008 to 2014	WET	ET	60.0	Hansen (2016) and López-Blanco et al. (2017)
GL-ZaF	74.48	-20.55	2008 to 2011	WET	ET	65.0	Lund et al. (2016a) and Soegaard (1999)
GL-ZaH	74.47	-20.55	2000 to 2014	GRA	ET	48.0	Lund et al. (2012 , 2016b)
IT-BCi	40.52	14.96	2004 to 2014	CRO	Csa	20.0	Magliulo et al. (2016) and Vitale et al. (2015)
IT-CA1	42.38	12.03	2011 to 2014	DBF	Csa	200.0	Sabbatini, Arriga, Bertolini, et al. (2016) and Sabbatini, Arriga, and Papale (2016)
IT-CA2	42.38	12.03	2011 to 2014	CRO	Csa	200.0	Sabbatini, Arriga, Bertolini, et al. (2016) and Sabbatini, Arriga, Gioli, and Papale (2016)
IT-CA3	42.38	12.02	2011 to 2014	DBF	Csa	197.0	Sabbatini, Arriga, Bertolini, et al. (2016) and Sabbatini, Arriga, Matteucci, and Papale (2016)
IT-Col	41.85	13.59	1996 to 2014	DBF	Cfb	1560.0	Matteucci (2016) and Valentini et al. (1996)

Continued on next page

Table S8 – *Continued from previous page*

Site ID	Lat	Lon	Obs. period	PFT	KG	Elev.	Reference
IT-Cp2	41.7	12.36	2012 to 2014	EBF	Csa	19.0	Fares et al. (2014) and Fares et al. (2016)
IT-Cpz	41.71	12.38	2000 to 2008	EBF	Csa	68.0	Garbulsky et al. (2008) and Valentini, Dore, et al. (2016)
IT-Isp	45.81	8.63	2013 to 2014	DBF	Cfa	210.0	Ferréa et al. (2012) and Gruening, Goded, Cescatti, and Pokorska (2016a)
IT-La2	45.95	11.29	2000 to 2002	ENF	Cfb	1350.0	Cescatti et al. (2016) and Marcolla et al. (2003)
IT-Lav	45.96	11.28	2003 to 2014	ENF	Cfb	1353.0	Gianelle, Zampedri, et al. (2016) and Marcolla et al. (2003)
IT-MBo	46.01	11.05	2003 to 2013	GRA	Dfb	1550.0	Gianelle, Cavagna, et al. (2016) and Marcolla et al. (2011)
IT-Noe	40.61	8.15	2004 to 2014	CSH	Csa	25.0	Marras et al. (2011) and Spano et al. (2016)
IT-PT1	45.2	9.06	2002 to 2004	DBF	Cfa	60.0	Manca and Goded (2016) and Migliavacca et al. (2009)
IT-Ren	46.59	11.43	1999 to 2013	ENF	Dfc	1730.0	Montagnani and Minerbi (2016) and Montagnani et al. (2009)

Continued on next page

Table S8 – *Continued from previous page*

Site ID	Lat	Lon	Obs. period	PFT	KG	Elev.	Reference
IT-Ro1	42.41	11.93	2000 to 2008	DBF	Csa	235.0	Rey et al. (2002) and Valentini, Tirone, et al. (2016)
IT-Ro2	42.39	11.92	2002 to 2012	DBF	Csa	224.0	Papale et al. (2016) and Tedeschi et al. (2005)
IT-SR2	43.73	10.29	2013 to 2014	ENF	Csa	4.0	Gruening, Goded, Cescatti, and Pokorska (2016b)
IT-SRo	43.73	10.28	1999 to 2012	ENF	Csa	4.0	Chiesi et al. (2005) and Gruening, Goded, Cescatti, Manca, and Seufert (2016)
IT-Tor	45.84	7.58	2008 to 2014	GRA	ET	2160.0	Cremonese et al. (2016) and Galvagno et al. (2013)
JP-MBF	44.39	142.32	2004 to 2005	DBF	Dfb	585.0	Kotani (2016a) and Matsumoto et al. (2008)
JP-SMF	35.26	137.08	2002 to 2006	MF	Cfa	205.0	Kotani (2016b) and Matsumoto et al. (2008)
NL-Hor	52.24	5.07	2004 to 2011	GRA	Cfb	-2.0	Dolman, Hendriks, et al. (2016) and Jacobs et al. (2007)
NL-Loo	52.17	5.74	1996 to 2014	ENF	Cfb	25.0	E. J. Moors (2012) and E. Moors and Elbers (2016)

Continued on next page

Table S8 – *Continued from previous page*

Site ID	Lat	Lon	Obs. period	PFT	KG	Elev.	Reference
PA-SPn	9.32	-79.63	2007 to 2009	DBF	Am	78.0	Wolf, Eugster, and Buchmann (2016a) and Wolf et al. (2011)
PA-SPs	9.31	-79.63	2007 to 2009	GRA	Am	68.0	Wolf, Eugster, and Buchmann (2016b) and Wolf et al. (2011)
RU-Che	68.61	161.34	2002 to 2005	WET	Dsc	6.0	Merbold, Kutsch, et al. (2009) and Merbold et al. (2016)
RU-Cok	70.83	147.49	2003 to 2013	OSH	Dfc	48.0	Dolman, Van Der Molen, et al. (2016) and Van der Molen et al. (2007)
RU-Fyo	56.46	32.92	1998 to 2014	ENF	Dfb	265.0	Kurbatova et al. (2008) and Varlagin et al. (2016)
RU-Hal	54.73	90.0	2002 to 2004	GRA	Dfb	446.0	Belelli et al. (2016) and Belelli Marchesini et al. (2007)
RU-Sam	72.37	126.5	2002 to 2014	GRA	Dsd	16.0	Boike et al. (2013) and Kutzbach et al. (2016)
RU-SkP	62.26	129.17	2012 to 2014	DNF	Dfd	246.0	Maximov (2016)
RU-Tks	71.59	128.89	2010 to 2014	GRA	Dsd	7.0	Aurela, Laurila, et al. (2016)
RU-Vrk	67.05	62.94	2008	CSH	Dfc	100.0	Friborg, Biasi, and Shurpali (2016)
SD-Dem	13.28	30.48	2005 to 2009	SAV	BWh	500.0	Ardö et al. (2008 , 2016)

Continued on next page

Table S8 – *Continued from previous page*

Site ID	Lat	Lon	Obs. period	PFT	KG	Elev.	Reference
SE-St1	68.35	19.05	2012 to 2014	WET	Dfc	351.0	Friborg, Jammet, and Crill (2016) and Jammet et al. (2015)
SJ-Adv	78.19	15.92	2012 to 2014	WET	ET	16.0	Christensen (2016)
SJ-Blv	78.92	11.83	2008 to 2009	SNO	ET	25.0	Boike et al. (2016) and Lüders et al. (2014)
SN-Dhr	15.4	-15.43	2010 to 2013	SAV	BWh	40.0	Tagesson et al. (2014, 2016)
US-AR1	36.43	-99.42	2009 to 2012	GRA	Cfa	611.0	D. Baldocchi and Penuelas (2019) and Billesbach et al. (2016a)
US-AR2	36.64	-99.6	2009 to 2012	GRA	Cfa	646.0	D. Baldocchi and Penuelas (2019) and Billesbach et al. (2016b)
US-ARB	35.55	-98.04	2005 to 2006	GRA	Cfa	424.0	Fischer et al. (2012) and Torn (2016a)
US-ARC	35.55	-98.04	2005 to 2006	GRA	Cfa	424.0	D. Baldocchi and Penuelas (2019) and Torn (2016b)
US-ARM	36.61	-97.49	2003 to 2012	CRO	Cfa	314.0	Bagley et al. (2017) and Biraud et al. (2016)
US-Atq	70.47	-157.41	2003 to 2008	WET	ET	15.0	Kwon et al. (2006) and Zona and Oechel (2016a)
US-Blo	38.9	-120.63	1997 to 2007	ENF	Csb	1315.0	B. Baker et al. (1999) and Goldstein (2016)

Continued on next page

Table S8 – *Continued from previous page*

Site ID	Lat	Lon	Obs. period	PFT	KG	Elev.	Reference
US-Cop	38.09	-109.39	2001 to 2007	GRA	BSk	1520.0	Bowling (2016) and Sullivan et al. (2019)
US-CRT	41.63	-83.35	2011 to 2013	CRO	Dfa	180.0	J. Chen and Chu (2016a) and Chu et al. (2018)
US-GBT	41.37	-106.24	2001 to 2003	ENF	Dfc	3191.0	D. Baldocchi and Penuelas (2019) and Massman (2016a)
US-GLE	41.37	-106.24	2005 to 2014	ENF	Dfc	3197.0	Arain and Restrepo-Coupe (2005) and Massman (2016b)
US-Goo	34.25	-89.87	2002 to 2006	GRA	Cfa	87.0	Meyers (2016) and Runkle et al. (2017)
US-Ha1	42.54	-72.17	1991 to 2012	DBF	Dfb	340.0	Antonarakis et al. (2017) and Munger (2016)
US-IB2	41.84	-88.24	2004 to 2011	GRA	Dfa	226.5	Allison et al. (2005) and Matamala (2016)
US-Ivo	68.49	-155.75	2004 to 2007	WET	ET	568.0	McEwing et al. (2015) and Zona and Oechel (2016b)
US-KS1	28.46	-80.67	2002	ENF	Cfa	1.0	Bracho et al. (2008) and Drake and Hinkle (2016a)
US-KS2	28.61	-80.67	2003 to 2006	CSH	Cfa	3.0	D. Baldocchi and Penuelas (2019) and Drake and Hinkle (2016b)
US-Lin	36.36	-119.84	2009 to 2010	CRO	BSk	131.0	Fares (2016) and Fares et al. (2013)

Continued on next page

Table S8 – *Continued from previous page*

Site ID	Lat	Lon	Obs. period	PFT	KG	Elev.	Reference
US-Los	46.08	-89.98	2000 to 2014	WET	Dfb	480.0	I. Baker et al. (2003) and A. Desai (2016a)
US-Me1	44.58	-121.5	2004 to 2005	ENF	Csb	896.0	D. Baldocchi and Penuelas (2019) and Law (2016a)
US-Me2	44.45	-121.56	2002 to 2014	ENF	Csb	1253.0	Campbell et al. (2004) and Law (2016b)
US-Me3	44.32	-121.61	2004 to 2009	ENF	Csb	1005.0	A. Barr et al. (2013) and Law (2016c)
US-Me4	44.5	-121.62	1996 to 2000	ENF	Csb	922.0	P. M. Anthoni et al. (1999) and Law (2016d)
US-Me5	44.44	-121.57	2000 to 2002	ENF	Csb	1188.0	P. M. Anthoni et al. (2002) and Law (2016e)
US-Me6	44.32	-121.61	2010 to 2014	ENF	Csb	998.0	Chu et al. (2018) and Law (2016f)
US-MMS	39.32	-86.41	1999 to 2014	DBF	Cfa	275.0	D. D. Baldocchi et al. (2005) and Novick and Phillips (2016)
US-Myb	38.05	-121.77	2011 to 2014	WET	Csa	-1.0	D. Baldocchi and Penuelas (2019) and Sturtevant et al. (2016)
US-Ne1	41.17	-96.48	2001 to 2013	CRO	Dfa	361.0	Amos et al. (2005) and Suyker (2016a)
US-Ne2	41.16	-96.47	2001 to 2013	CRO	Dfa	362.0	Amos et al. (2005) and Suyker (2016b)
US-Ne3	41.18	-96.44	2001 to 2013	CRO	Dfa	363.0	Amos et al. (2005) and Suyker (2016c)

Continued on next page

Table S8 – *Continued from previous page*

Site ID	Lat	Lon	Obs. period	PFT	KG	Elev.	Reference
US-NR1	40.03	-105.55	1999 to 2014	ENF	Dfc	3050.0	Albert et al. (2017) and Blanken et al. (2016)
US-Oho	41.55	-83.84	2004 to 2013	DBF	Dfa	230.0	J. Chen et al. (2016) and Chu et al. (2018)
US-ORv	40.02	-83.02	2011	WET	Cfa	221.0	Bohrer (2016) and Brooker et al. (2014)
US-PFa	45.95	-90.27	1996 to 2014	MF	Dfb	470.0	A. Desai (2016b) and Keppel-Aleks et al. (2012)
US-Prr	65.12	-147.49	2010 to 2014	ENF	Dfc	210.0	Ikawa et al. (2015) and Kobayashi and Suzuki (2016)
US-SRC	31.91	-110.84	2008 to 2014	OSH	BSh	991.0	Kurc (2016) and Wolf, Keenan, et al. (2016)
US-SRG	31.79	-110.83	2008 to 2014	GRA	Csa	1291.0	D. Baldocchi and Penuelas (2019) and Scott (2016b)
US-SRM	31.82	-110.87	2004 to 2014	WSA	BSk	1120.0	Barron-Gafford et al. (2013) and Scott (2016c)
US-Sta	41.4	-106.8	2005 to 2009	OSH	Dfb	2069.0	Ewers and Pendall (2016) and Reed et al. (2018)
US-Syv	46.24	-89.35	2001 to 2014	MF	Dfb	540.0	A. Barr et al. (2013) and A. Desai (2016c)
US-Ton	38.43	-120.97	2001 to 2014	WSA	Csa	177.0	D. Baldocchi and Ma (2016) and D. D. Bal- docchi et al. (2010)

Continued on next page

Table S8 – *Continued from previous page*

Site ID	Lat	Lon	Obs. period	PFT	KG	Elev.	Reference
US-Tw1	38.11	-121.65	2012 to 2014	WET	Csa	-9.0	D. Baldocchi and Penuelas (2019) and Szutu et al. (2016)
US-Tw2	38.1	-121.64	2012 to 2013	CRO	Csa	-5.0	D. Baldocchi (2016a) and D. Baldocchi and Penuelas (2019)
US-Tw3	38.12	-121.65	2013 to 2014	CRO	Csa	-9.0	D. Baldocchi and Penuelas (2019) and Szutu and Baldocchi (2016)
US-Tw4	38.1	-121.64	2013 to 2014	WET	Csa	-5.0	Chamberlain et al. (2017) and Sanchez et al. (2016)
US-Twt	38.11	-121.65	2009 to 2014	CRO	Csa	-7.0	D. Baldocchi (2016b) and D. Baldocchi and Penuelas (2019)
US-UMB	45.56	-84.71	2000 to 2014	DBF	Dfb	234.0	Aron et al. (2019) and Gough et al. (2016a)
US-UMd	45.56	-84.7	2007 to 2014	DBF	Dfb	239.0	Atkins et al. (2018) and Gough et al. (2016b)
US-Var	38.41	-120.95	2000 to 2014	GRA	Csa	129.0	D. Baldocchi et al. (2016) and D. D. Baldocchi et al. (2004)
US-WCr	45.81	-90.08	1999 to 2014	DBF	Dfb	520.0	I. Baker et al. (2003) and A. Desai (2016d)
US-Whs	31.74	-110.05	2007 to 2014	OSH	BSk	1370.0	Biederman et al. (2017) and Scott (2016a)

Continued on next page

Table S8 – *Continued from previous page*

Site ID	Lat	Lon	Obs. period	PFT	KG	Elev.	Reference
US-Wi0	46.62	-91.08	2002	ENF	Dfb	349.0	J. Chen (2016a) and Chu et al. (2018)
US-Wi1	46.73	-91.23	2003	DBF	Dfb	352.0	J. Chen (2016b) and Chu et al. (2018)
US-Wi2	46.69	-91.15	2003	ENF	Dfb	395.0	J. Chen (2016c) and A. R. Desai et al. (2008)
US-Wi3	46.63	-91.1	2002 to 2004	DBF	Dfb	411.0	J. Chen (2016d) and Chu et al. (2018)
US-Wi4	46.74	-91.17	2002 to 2005	ENF	Dfb	352.0	J. Chen (2016e) and Chu et al. (2018)
US-Wi5	46.65	-91.09	2004	ENF	Dfb	353.0	J. Chen (2016f) and Chu et al. (2018)
US-Wi6	46.62	-91.3	2002 to 2003	OSH	Dfb	371.0	J. Chen (2016g) and A. R. Desai et al. (2008)
US-Wi7	46.65	-91.07	2005	OSH	Dfb	335.0	J. Chen (2016h) and Chu et al. (2021)
US-Wi8	46.72	-91.25	2002	DBF	Dfb	348.0	J. Chen (2016i) and Chu et al. (2018)
US-Wi9	46.62	-91.08	2004 to 2005	ENF	Dfb	350.0	J. Chen (2016j) and Chu et al. (2018)
US-Wkg	31.74	-109.94	2004 to 2014	GRA	BSk	1531.0	Biederman et al. (2017) and Scott (2016d)
US-WPT	41.46	-83.0	2011 to 2013	WET	Cfa	175.0	J. Chen and Chu (2016b) and Chu et al. (2016)
ZA-Kru	-25.02	31.5	2000 to 2013	SAV	BSh	359.0	Archibald et al. (2009) and Scholes (2016)

Continued on next page

Table S8 – *Continued from previous page*

Site ID	Lat	Lon	Obs. period	PFT	KG	Elev.	Reference
ZM-Mon	-15.44	23.25	2000 to 2009	DBF	Aw	1053.0	Kutsch et al. (2016) and Merbold, Ardö, et al. (2009)

References

- Acosta, M., Pavelka, M., Montagnani, L., Kutsch, W., Lindroth, A., Juszczak, R., & Janouš, D. (2013). Soil surface CO₂ efflux measurements in Norway spruce forests: Comparison between four different sites across Europe – from boreal to alpine forest. *Geoderma*, 192, 295–303. <https://doi.org/10.1016/j.geoderma.2012.08.027>
- Albert, L. P., Keenan, T. F., Burns, S. P., Huxman, T. E., & Monson, R. K. (2017). Climate controls over ecosystem metabolism: insights from a fifteen-year inductive artificial neural network synthesis for a subalpine forest. *Oecologia*, 184(1), 25–41. <https://doi.org/10.1007/s00442-017-3853-0>
- Allison, V. J., Miller, R. M., Jastrow, J. D., Matamala, R., & Zak, D. R. (2005). Changes in Soil Microbial Community Structure in a Tallgrass Prairie Chronosequence. *Soil Science Society of America Journal*, 69(5), 1412–1421. <https://doi.org/10.2136/sssaj2004.0252>
- Amiro, B. (2009). Measuring boreal forest evapotranspiration using the energy balance residual. *Journal of Hydrology*, 366(1–4), 112–118. <https://doi.org/10.1016/j.jhydrol.2008.12.021>
- Amiro, B. (2016a). FLUXNET2015 CA-SF1 Saskatchewan - Western Boreal, forest burned in 1977. <https://doi.org/10.18140/FLX/1440046>
- Amiro, B. (2016b). FLUXNET2015 CA-SF2 Saskatchewan - Western Boreal, forest burned in 1989. <https://doi.org/10.18140/FLX/1440047>
- Amiro, B. (2016c). FLUXNET2015 CA-SF3 Saskatchewan - Western Boreal, forest burned in 1998. <https://doi.org/10.18140/FLX/1440048>
- Ammann, C., Spirig, C., Leifeld, J., & Neftel, A. (2009). Assessment of the nitrogen and carbon budget of two managed temperate grassland fields. *Agriculture, Ecosystems & Environment*, 133(3–4), 150–162. <https://doi.org/10.1016/j.agee.2009.05.006>
- Ammann, C. (2016). FLUXNET2015 CH-Oe1 Oensingen grassland. <https://doi.org/10.18140/FLX/1440135>
- Amos, B., Arkebauer, T. J., & Doran, J. W. (2005). Soil Surface Fluxes of Greenhouse Gases in an Irrigated Maize-Based Agroecosystem. *Soil Science Society of America Journal*, 69(2), 387–395. <https://doi.org/10.2136/sssaj2005.0387>
- Anthoni, P. M., Knohl, A., Rebmann, C., Freibauer, A., Mund, M., Ziegler, W., Kolle, O., & Schulze, E.-D. (2004). Forest and agricultural land-use-dependent CO₂ exchange in Thuringia, Germany. *Global Change Biology*, 10(12), 2005–2019. <https://doi.org/10.1111/j.1365-2486.2004.00863.x>

- Anthoni, P. M., Law, B. E., & Unsworth, M. H. (1999). Carbon and water vapor exchange of an open-canopied ponderosa pine ecosystem. *Agricultural and Forest Meteorology*, 95(3), 151–168. [https://doi.org/10.1016/s0168-1923\(99\)00029-5](https://doi.org/10.1016/s0168-1923(99)00029-5)
- Anthoni, P. M., Unsworth, M. H., Law, B. E., Irvine, J., Baldocchi, D. D., Tuyl, S. V., & Moore, D. (2002). Seasonal differences in carbon and water vapor exchange in young and old-growth ponderosa pine ecosystems. *Agricultural and Forest Meteorology*, 111(3), 203–222. [https://doi.org/10.1016/s0168-1923\(02\)00021-7](https://doi.org/10.1016/s0168-1923(02)00021-7)
- Antonarakis, A. S., Siqueira, P., & Munger, J. W. (2017). Using multi-source data from lidar, radar, imaging spectroscopy, and national forest inventories to simulate forest carbon fluxes. *International Journal of Remote Sensing*, 38(19), 5464–5486. <https://doi.org/10.1080/01431161.2017.1341666>
- Arain, M. A. (2016a). FLUXNET2015 CA-TP1 Ontario - Turkey Point 2002 Plantation White Pine. <https://doi.org/10.18140/FLX/1440050>
- Arain, M. A. (2016b). FLUXNET2015 CA-TP2 Ontario - Turkey Point 1989 Plantation White Pine. <https://doi.org/10.18140/FLX/1440051>
- Arain, M. A. (2016c). FLUXNET2015 CA-TP3 Ontario - Turkey Point 1974 Plantation White Pine. <https://doi.org/10.18140/FLX/1440052>
- Arain, M. A. (2016d). FLUXNET2015 CA-TP4 Ontario - Turkey Point 1939 Plantation White Pine. <https://doi.org/10.18140/FLX/1440053>
- Arain, M. A. (2016e). FLUXNET2015 CA-TPD Ontario - Turkey Point Mature Deciduous. <https://doi.org/10.18140/FLX/1440112>
- Arain, M. A., & Restrepo-Coupe, N. (2005). Net ecosystem production in a temperate pine plantation in southeastern Canada. *Agricultural and Forest Meteorology*, 128(3–4), 223–241. <https://doi.org/10.1016/j.agrformet.2004.10.003>
- Archibald, S. A., Kirton, A., van der Merwe, M. R., Scholes, R. J., Williams, C. A., & Hanan, N. (2009). Drivers of inter-annual variability in Net Ecosystem Exchange in a semi-arid savanna ecosystem, South Africa. *Biogeosciences*, 6(2), 251–266. <https://doi.org/10.5194/bg-6-251-2009>
- Ardö, J., El Tahir, B. A., & ElKhidir, H. A. M. (2016). FLUXNET2015 SD-Dem Demokeya. <https://doi.org/10.18140/FLX/1440186>
- Ardö, J., Mölder, M., El-Tahir, B. A., & Elkhidir, H. A. M. (2008). Seasonal variation of carbon fluxes in a sparse savanna in semi arid Sudan. *Carbon Balance and Management*, 3(1). <https://doi.org/10.1186/1750-0680-3-7>

- Arndt, S., Hinko-Najera, N., & Griebel, A. (2016). FLUXNET2015 AU-Wom Wombat. <https://doi.org/10.18140/FLX/1440207>
- Aron, P. G., Poulsen, C. J., Fiorella, R. P., & Matheny, A. M. (2019). Stable Water Isotopes Reveal Effects of Intermediate Disturbance and Canopy Structure on Forest Water Cycling. *Journal of Geophysical Research: Biogeosciences*, 124(10), 2958–2975. <https://doi.org/10.1029/2019jg005118>
- Asner, G. P., Keller, M., Pereira, R., Jr, Zweede, J. C., & Silva, J. N. M. (2004). Canopy damage and recovery after selective logging in Amazonia: field and satellite studies. *Ecological Applications*, 14(sp4), 280–298. <https://doi.org/10.1890/01-6019>
- Atkins, J. W., Bohrer, G., Fahey, R. T., Hardiman, B. S., Morin, T. H., Stovall, A. E. L., Zimmerman, N., & Gough, C. M. (2018). Quantifying vegetation and canopy structural complexity from terrestrial LiDAR data using the forestr r package (Goslee, Sarah, Ed.). *Methods in Ecology and Evolution*, 9(10), 2057–2066. <https://doi.org/10.1111/2041-210x.13061>
- Aubinet, M., Chermanne, B., Vandenhaut, M., Longdoz, B., Yernaux, M., & Laitat, E. (2001). Long term carbon dioxide exchange above a mixed forest in the Belgian Ardennes. *Agricultural and Forest Meteorology*, 108(4), 293–315. [https://doi.org/10.1016/s0168-1923\(01\)00244-1](https://doi.org/10.1016/s0168-1923(01)00244-1)
- Aurela, M., Laurila, T., Hatakka, J., Tuovinen, J.-P., & Rainne, J. (2016). FLUXNET2015 RU-Tks Tiksi. <https://doi.org/10.18140/FLX/1440244>
- Aurela, M., Lohila, A., Tuovinen, J.-P., Hatakka, J., Penttila, T., & Laurila, T. (2015). Carbon dioxide and energy flux measurements in four northern-boreal ecosystems at pallas [4th Pallas Symposium 2013, Muonio, Finland, Sep 25-27, 2013]. *Boreal Environment Research*, 20(4), 455–473. <https://helda.helsinki.fi/bitstreams/4cfcb066-087c-4586-8933-6b16c4a266c2/download>
- Aurela, M., Lohila, A., Tuovinen, J.-P., Hatakka, J., Rainne, J., Mäkelä, T., & Lauria, T. (2016). FLUXNET2015 FI-Lom Lompolojankka. <https://doi.org/10.18140/FLX/1440228>
- Aurela, M., Tuovinen, J.-P., Hatakka, J., Lohila, A., Mäkelä, T., Rainne, J., & Lauria, T. (2016). FLUXNET2015 FI-Sod Sodankyla. <https://doi.org/10.18140/FLX/1440160>
- Bagley, J. E., Kueppers, L. M., Billesbach, D. P., Williams, I. N., Biraud, S. C., & Torn, M. S. (2017). The influence of land cover on surface energy partitioning and evaporative fraction regimes in the U.S. Southern Great Plains. *Journal of Geophysical Research: Atmospheres*, 122(11), 5793–5807. <https://doi.org/10.1002/2017jd026740>
- Baker, B., Guenther, A., Greenberg, J., Goldstein, A., & Fall, R. (1999). Canopy fluxes of 2-methyl-3-butene-2-ol over a ponderosa pine forest by relaxed eddy accumulation: Field data and

- model comparison. *Journal of Geophysical Research: Atmospheres*, 104(D21), 26107–26114. <https://doi.org/10.1029/1999jd900749>
- Baker, I., Denning, A. S., Hanan, N., Prihodko, L., Uliasz, M., Vidale, P.-L., Davis, K., & Bakwin, P. (2003). Simulated and observed fluxes of sensible and latent heat and CO₂ at the WLEF-TV tower using SiB2.5. *Global Change Biology*, 9(9), 1262–1277. <https://doi.org/10.1046/j.1365-2486.2003.00671.x>
- Baker, T. R., Phillips, O. L., Malhi, Y., Almeida, S., Arroyo, L., Di Fiore, A., Erwin, T., Killeen, T. J., Laurance, S. G., Laurance, W. F., Lewis, S. L., Lloyd, J., Monteagudo, A., Neill, D. A., Patiño, S., Pitman, N. C. A., M. Silva, J. N., & Vásquez Martínez, R. (2004). Variation in wood density determines spatial patterns in Amazonian forest biomass. *Global Change Biology*, 10(5), 545–562. <https://doi.org/10.1111/j.1365-2486.2004.00751.x>
- Baldocchi, D. (2016a). FLUXNET2015 US-Tw2 Twitchell Corn. <https://doi.org/10.18140/FLX/1440109>
- Baldocchi, D. (2016b). FLUXNET2015 US-Twt Twitchell Island. <https://doi.org/10.18140/FLX/1440106>
- Baldocchi, D., & Ma, S. (2016). FLUXNET2015 US-Ton Tonzi Ranch. <https://doi.org/10.18140/FLX/1440092>
- Baldocchi, D., Ma, S., & Xu, L. (2016). FLUXNET2015 US-Var Vaira Ranch- Ione. <https://doi.org/10.18140/FLX/1440094>
- Baldocchi, D., & Penuelas, J. (2019). The physics and ecology of mining carbon dioxide from the atmosphere by ecosystems. *Global Change Biology*, 25(4), 1191–1197. <https://doi.org/10.1111/gcb.14559>
- Baldocchi, D. D., Black, T. A., Curtis, P. S., Falge, E., Fuentes, J. D., Granier, A., Gu, L., Knohl, A., Pilegaard, K., Schmid, H. P., Valentini, R., Wilson, K., Wofsy, S., Xu, L., & Yamamoto, S. (2005). Predicting the onset of net carbon uptake by deciduous forests with soil temperature and climate data: a synthesis of FLUXNET data. *International Journal of Biometeorology*, 49(6), 377–387. <https://doi.org/10.1007/s00484-005-0256-4>
- Baldocchi, D. D., Ma, S., Rambal, S., Misson, L., Ourcival, J.-M., Limousin, J.-M., Pereira, J., & Papale, D. (2010). On the differential advantages of evergreenness and deciduousness in mediterranean oak woodlands: a flux perspective. *Ecological Applications*, 20(6), 1583–1597. <https://doi.org/10.1890/08-2047.1>
- Baldocchi, D. D., Xu, L., & Kiang, N. (2004). How plant functional-type, weather, seasonal drought, and soil physical properties alter water and energy fluxes of an oak–grass savanna and an

- annual grassland. *Agricultural and Forest Meteorology*, 123(1–2), 13–39. <https://doi.org/10.1016/j.agrformet.2003.11.006>
- Bao, S., Alonso, L., Wang, S., Gensheimer, J., De, R., & Carvalhais, N. (2023). Toward robust parameterizations in ecosystem-level photosynthesis models. *Journal of Advances in Modeling Earth Systems*, 15(8), e2022MS003464. <https://doi.org/10.1029/2022MS003464>
- Bao, S., Wutzler, T., Koirala, S., Cuntz, M., Ibrom, A., Besnard, S., Walther, S., Šigut, L., Moreno, A., Weber, U., Wohlfahrt, G., Cleverly, J., Migliavacca, M., Woodgate, W., Merbold, L., Veenendaal, E., & Carvalhais, N. (2022). Environment-sensitivity functions for gross primary productivity in light use efficiency models. *Agricultural and Forest Meteorology*, 312, 108708. <https://doi.org/10.1016/j.agrformet.2021.108708>
- Barr, A., Richardson, A., Hollinger, D., Papale, D., Arain, M., Black, T., Bohrer, G., Dragoni, D., Fischer, M., Gu, L., Law, B., Margolis, H., McCaughey, J., Munger, J., Oechel, W., & Schaeffer, K. (2013). Use of change-point detection for friction–velocity threshold evaluation in eddy-covariance studies. *Agricultural and Forest Meteorology*, 171–172, 31–45. <https://doi.org/10.1016/j.agrformet.2012.11.023>
- Barr, A. G., Black, T., Hogg, E., Kljun, N., Morgenstern, K., & Nesic, Z. (2004). Inter-annual variability in the leaf area index of a boreal aspen-hazelnut forest in relation to net ecosystem production. *Agricultural and Forest Meteorology*, 126(3–4), 237–255. <https://doi.org/10.1016/j.agrformet.2004.06.011>
- Barron-Gafford, G. A., Scott, R. L., Jenerette, G. D., Hamerlynck, E. P., & Huxman, T. E. (2013). Landscape and environmental controls over leaf and ecosystem carbon dioxide fluxes under woody plant expansion (Turnbull, Matthew, Ed.). *Journal of Ecology*, 101(6), 1471–1483. <https://doi.org/10.1111/1365-2745.12161>
- Bazot, S., Barthes, L., Blanot, D., & Fresneau, C. (2013). Distribution of non-structural nitrogen and carbohydrate compounds in mature oak trees in a temperate forest at four key phenological stages. *Trees*, 27(4), 1023–1034. <https://doi.org/10.1007/s00468-013-0853-5>
- Beck, H. E., Zimmermann, N. E., McVicar, T. R., Vergopolan, N., Berg, A., & Wood, E. F. (2018). Present and future Köppen-Geiger climate classification maps at 1-km resolution. *Scientific Data*, 5(1), 180214. <https://doi.org/10.1038/sdata.2018.214>
- Belelli, L., Papale, D., & Valentini, R. (2016). FLUXNET2015 RU-Ha1 Hakasia steppe. <https://doi.org/10.18140/FLX/1440184>
- Belelli Marchesini, L., Papale, D., Reichstein, M., Vuichard, N., Tchebakova, N., & Valentini, R. (2007). Carbon balance assessment of a natural steppe of southern siberia by multiple constraint approach. *Biogeosciences*, 4(4), 581–595. <https://doi.org/10.5194/bg-4-581-2007>

- Berbigier, P., Bonnefond, J.-M., & Mellmann, P. (2001). CO₂ and water vapour fluxes for 2 years above Euroflux forest site. *Agricultural and Forest Meteorology*, 108(3), 183–197. [https://doi.org/10.1016/s0168-1923\(01\)00240-4](https://doi.org/10.1016/s0168-1923(01)00240-4)
- Berbigier, P., & Loustau, D. (2016). FLUXNET2015 FR-LBr Le Bray. <https://doi.org/10.18140/FLX/1440163>
- Beringer, J., Cunningham, S., Baker, P., Cavagnaro, T., MacNally, R., Thompson, R., & McHugh, I. (2016). FLUXNET2015 AU-Whr Whroo. <https://doi.org/10.18140/FLX/1440206>
- Beringer, J., Hacker, J., Hutley, L. B., Leuning, R., Arndt, S. K., Amiri, R., Bannehr, L., Cernusak, L. A., Grover, S., Hensley, C., Hocking, D., Isaac, P., Jamali, H., Kanniah, K., Livesley, S., Neininger, B., Paw U, K. T., Sea, W., Straten, D., ... Zegelin, S. (2011). SPECIAL—Savanna Patterns of Energy and Carbon Integrated across the Landscape. *Bulletin of the American Meteorological Society*, 92(11), 1467–1485. <https://doi.org/10.1175/2011bams2948.1>
- Beringer, J., & Hutley, L. (2016a). FLUXNET2015 AU-Ade Adelaide River. <https://doi.org/10.18140/FLX/1440193>
- Beringer, J., & Hutley, L. (2016b). FLUXNET2015 AU-DaP Daly River Savanna. <https://doi.org/10.18140/FLX/1440123>
- Beringer, J., & Hutley, L. (2016c). FLUXNET2015 AU-DaS Daly River Cleared. <https://doi.org/10.18140/FLX/1440122>
- Beringer, J., & Hutley, L. (2016d). FLUXNET2015 AU-Dry Dry River. <https://doi.org/10.18140/FLX/1440197>
- Beringer, J., & Hutley, L. (2016e). FLUXNET2015 AU-Fog Fogg Dam. <https://doi.org/10.18140/FLX/1440124>
- Beringer, J., & Hutley, L. (2016f). FLUXNET2015 AU-RDF Red Dirt Melon Farm, Northern Territory. <https://doi.org/10.18140/FLX/1440201>
- Beringer, J., Hutley, L., McGuire, D., & U, P. (2016). FLUXNET2015 AU-Wac Wallaby Creek. <https://doi.org/10.18140/FLX/1440127>
- Beringer, J., Hutley, L. B., Hacker, J. M., Neininger, B., & Paw U, K. T. (2011). Patterns and processes of carbon, water and energy cycles across northern Australian landscapes: From point to region. *Agricultural and Forest Meteorology*, 151(11), 1409–1416. <https://doi.org/10.1016/j.agrformet.2011.05.003>
- Beringer, J., Hutley, L. B., McHugh, I., Arndt, S. K., Campbell, D., Cleugh, H. A., Cleverly, J., Resco de Dios, V., Eamus, D., Evans, B., Ewenz, C., Grace, P., Griebel, A., Haverd, V., Hinko-Najera, N., Huete, A., Isaac, P., Kanniah, K., Leuning, R., ... Wardlaw, T. (2016). An intro-

- duction to the Australian and New Zealand flux tower network – OzFlux. *Biogeosciences*, 13(21), 5895–5916. <https://doi.org/10.5194/bg-13-5895-2016>
- Beringer, J., Livesley, S. J., Randle, J., & Hutley, L. B. (2013). Carbon dioxide fluxes dominate the greenhouse gas exchanges of a seasonal wetland in the wet-dry tropics of northern Australia. *Agricultural and Forest Meteorology*, 182–183, 239–247. <https://doi.org/10.1016/j.agrformet.2013.06.008>
- Beringer, J., & Walker, J. (2016). FLUXNET2015 AU-Ync Jaxa. <https://doi.org/10.18140/FLX/1440208>
- Bernhofer, C., Grünwald, T., Moderow, U., Hehn, M., Eichelmann, U., & Prasse, H. (2016a). FLUXNET2015 DE-Akm Anklam. <https://doi.org/10.18140/FLX/1440213>
- Bernhofer, C., Grünwald, T., Moderow, U., Hehn, M., Eichelmann, U., & Prasse, H. (2016b). FLUXNET2015 DE-Gri Grillenburg. <https://doi.org/10.18140/FLX/1440147>
- Bernhofer, C., Grünwald, T., Moderow, U., Hehn, M., Eichelmann, U., & Prasse, H. (2016c). FLUXNET2015 DE-Kli Klingenberg. <https://doi.org/10.18140/FLX/1440149>
- Bernhofer, C., Grünwald, T., Moderow, U., Hehn, M., Eichelmann, U., & Prasse, H. (2016d). FLUXNET2015 DE-Obe Oberbärenburg. <https://doi.org/10.18140/FLX/1440151>
- Bernhofer, C., Grünwald, T., Moderow, U., Hehn, M., Eichelmann, U., & Prasse, H. (2016e). FLUXNET2015 DE-Spw Spreewald. <https://doi.org/10.18140/FLX/1440220>
- Bernhofer, C., Grünwald, T., Moderow, U., Hehn, M., Eichelmann, U., & Prasse, H. (2016f). FLUXNET2015 DE-Tha Tharandt. <https://doi.org/10.18140/FLX/1440152>
- Berveiller, D., Delpierre, N., Dufrêne, E., Pontailler, J.-Y., Vanbostal, L., Janvier, B., Mottet, L., & Cristinacce, K. (2016). FLUXNET2015 FR-Fon Fontainebleau-Barbeau. <https://doi.org/10.18140/FLX/1440161>
- Biedermaier, J. A., Scott, R. L., Bell, T. W., Bowling, D. R., Dore, S., Garatuza-Payan, J., Kolb, T. E., Krishnan, P., Krofcheck, D. J., Litvak, M. E., Maurer, G. E., Meyers, T. P., Oechel, W. C., Papuga, S. A., Ponce-Campos, G. E., Rodriguez, J. C., Smith, W. K., Vargas, R., Watts, C. J., ... Goulden, M. L. (2017). CO₂ exchange and evapotranspiration across dryland ecosystems of southwestern North America. *Global Change Biology*, 23(10), 4204–4221. <https://doi.org/10.1111/gcb.13686>
- Billesbach, D., Bradford, J., & Torn, M. (2016a). FLUXNET2015 US-AR1 ARM USDA UNL OSU Woodward Switchgrass 1. <https://doi.org/10.18140/FLX/1440103>
- Billesbach, D., Bradford, J., & Torn, M. (2016b). FLUXNET2015 US-AR2 ARM USDA UNL OSU Woodward Switchgrass 2. <https://doi.org/10.18140/FLX/1440104>

- Biraud, S., Fischer, M., Chan, S., & Torn, M. (2016). FLUXNET2015 US-ARM ARM Southern Great Plains site- Lamont. <https://doi.org/10.18140/FLX/1440066>
- Black, T. A. (2016a). FLUXNET2015 CA-Oas Saskatchewan - Western Boreal, Mature Aspen. <https://doi.org/10.18140/FLX/1440043>
- Black, T. A. (2016b). FLUXNET2015 CA-Obs Saskatchewan - Western Boreal, Mature Black Spruce. <https://doi.org/10.18140/FLX/1440044>
- Blanken, P. D., Monson, R. K., Burns, S. P., Bowling, D. R., & Turnipseed, A. A. (2016). FLUXNET2015 US-NR1 Niwot Ridge Forest (LTER NWT1). <https://doi.org/10.18140/FLX/1440087>
- Bohrer, G. (2016). FLUXNET2015 US-ORv Olentangy River Wetland Research Park. <https://doi.org/10.18140/FLX/1440102>
- Boike, J., Kattenstroth, B., Abramova, K., Bornemann, N., Chetverova, A., Fedorova, I., Fröb, K., Grigoriev, M., Grüber, M., Kutzbach, L., Langer, M., Minke, M., Muster, S., Piel, K., Pfeiffer, E.-M., Stoof, G., Westermann, S., Wischnewski, K., Wille, C., & Hubberten, H.-W. (2013). Baseline characteristics of climate, permafrost and land cover from a new permafrost observatory in the Lena River Delta, Siberia (1998–2011). *Biogeosciences*, 10(3), 2105–2128. <https://doi.org/10.5194/bg-10-2105-2013>
- Boike, J., Westermann, S., Lüers, J., Langer, M., & Piel, K. (2016). FLUXNET2015 SJ-Blv Bayelva, Spitsbergen. <https://doi.org/10.18140/FLX/1440242>
- Bonal, D., Bosc, A., Ponton, S., Goret, J.-Y., Burban, B., Gross, P., Bonnefond, J.-M., Elbers, J., Longdoz, B., Epron, D., Guehl, J.-M., & Granier, A. (2008). Impact of severe dry season on net ecosystem exchange in the Neotropical rainforest of French Guiana. *Global Change Biology*, 14(8), 1917–1933. <https://doi.org/10.1111/j.1365-2486.2008.01610.x>
- Bonal, D., & Burban, B. (2016). FLUXNET2015 GF-Guy Guyaflux (French Guiana). <https://doi.org/10.18140/FLX/1440165>
- Bowling, D. (2016). FLUXNET2015 US-Cop Corral Pocket. <https://doi.org/10.18140/FLX/1440100>
- Bracho, R., Powell, T. L., Dore, S., Li, J., Hinkle, C. R., & Drake, B. G. (2008). Environmental and biological controls on water and energy exchange in Florida scrub oak and pine flatwoods ecosystems. *Journal of Geophysical Research: Biogeosciences*, 113(G2). <https://doi.org/10.1029/2007jg000469>
- Bristow, M., Hutley, L. B., Beringer, J., Livesley, S. J., Edwards, A. C., & Arndt, S. K. (2016). Quantifying the relative importance of greenhouse gas emissions from current and future savanna land use change across northern Australia. *Biogeosciences*, 13(22), 6285–6303. <https://doi.org/10.5194/bg-13-6285-2016>

- Brooker, M. R., Bohrer, G., & Mouser, P. J. (2014). Variations in potential CH₄ flux and CO₂ respiration from freshwater wetland sediments that differ by microsite location, depth and temperature. *Ecological Engineering*, 72, 84–94. <https://doi.org/10.1016/j.ecoleng.2014.05.028>
- Brümmer, C., Lucas-Moffat, A. M., Herbst, M., & Kolle, O. (2016). FLUXNET2015 DE-Geb Gebe-see. <https://doi.org/10.18140/FLX/1440146>
- Buysse, P., Durand, B., Gueudet, J.-C., Mascher, N., Larmanou, E., Cellier, P., & Loubet, B. (2016). FLUXNET2015 FR-Gri Grignon. <https://doi.org/10.18140/FLX/1440162>
- Campbell, J. L., Sun, O. J., & Law, B. E. (2004). Disturbance and net ecosystem production across three climatically distinct forest landscapes. *Global Biogeochemical Cycles*, 18(4). <https://doi.org/10.1029/2004gb002236>
- Cañete, E. P. S., Ortiz, P. S., Jiménez, M. R. M., Poveda, F. D., Priego, O. P., Ballesteros, A. L., & Kowalski, A. S. (2016). FLUXNET2015 ES-LJu Llano de los Juanes. <https://doi.org/10.18140/FLX/1440157>
- Carrara, A., Janssens, I. A., Curiel Yuste, J., & Ceulemans, R. (2004). Seasonal changes in photosynthesis, respiration and NEE of a mixed temperate forest. *Agricultural and Forest Meteorology*, 126(1–2), 15–31. <https://doi.org/10.1016/j.agrformet.2004.05.002>
- Cernusak, L. A., Hutley, L. B., Beringer, J., Holtum, J. A., & Turner, B. L. (2011). Photosynthetic physiology of eucalypts along a sub-continental rainfall gradient in northern Australia. *Agricultural and Forest Meteorology*, 151(11), 1462–1470. <https://doi.org/10.1016/j.agrformet.2011.01.006>
- Cescatti, A., Marcolla, B., Zorer, R., & Gianelle, D. (2016). FLUXNET2015 IT-La2 Lavarone2. <https://doi.org/10.18140/FLX/1440235>
- Chamberlain, S. D., Verfaillie, J., Eichelmann, E., Hemes, K. S., & Baldocchi, D. D. (2017). Evaluation of Density Corrections to Methane Fluxes Measured by Open-Path Eddy Covariance over Contrasting Landscapes. *Boundary-Layer Meteorology*, 165(2), 197–210. <https://doi.org/10.1007/s10546-017-0275-9>
- Chen, J. (2016a). FLUXNET2015 US-Wi0 Young red pine (YRP). <https://doi.org/10.18140/FLX/1440055>
- Chen, J. (2016b). FLUXNET2015 US-Wi1 Intermediate hardwood (IHW). <https://doi.org/10.18140/FLX/1440054>
- Chen, J. (2016c). FLUXNET2015 US-Wi2 Intermediate red pine (IRP). <https://doi.org/10.18140/FLX/1440056>
- Chen, J. (2016d). FLUXNET2015 US-Wi3 Mature hardwood (MHW). <https://doi.org/10.18140/FLX/1440057>

- Chen, J. (2016e). FLUXNET2015 US-Wi4 Mature red pine (MRP). <https://doi.org/10.18140/FLX/1440058>
- Chen, J. (2016f). FLUXNET2015 US-Wi5 Mixed young jack pine (MYJP). <https://doi.org/10.18140/FLX/1440059>
- Chen, J. (2016g). FLUXNET2015 US-Wi6 Pine barrens #1 (PB1). <https://doi.org/10.18140/FLX/1440060>
- Chen, J. (2016h). FLUXNET2015 US-Wi7 Red pine clearcut (RPCC). <https://doi.org/10.18140/FLX/1440061>
- Chen, J. (2016i). FLUXNET2015 US-Wi8 Young hardwood clearcut (YHW). <https://doi.org/10.18140/FLX/1440062>
- Chen, J. (2016j). FLUXNET2015 US-Wi9 Young Jack pine (YJP). <https://doi.org/10.18140/FLX/1440063>
- Chen, J., & Chu, H. (2016a). FLUXNET2015 US-CRT Curtice Walter-Berger cropland. <https://doi.org/10.18140/FLX/1440117>
- Chen, J., & Chu, H. (2016b). FLUXNET2015 US-WPT Winous Point North Marsh. <https://doi.org/10.18140/FLX/1440116>
- Chen, J., Chu, H., & Noormets, A. (2016). FLUXNET2015 US-Oho Oak Openings. <https://doi.org/10.18140/FLX/1440088>
- Chen, S. (2016). FLUXNET2015 CN-Du2 Duolun grassland (D01). <https://doi.org/10.18140/FLX/1440140>
- Chen, S., Chen, J., Lin, G., Zhang, W., Miao, H., Wei, L., Huang, J., & Han, X. (2009). Energy balance and partition in Inner Mongolia steppe ecosystems with different land use types. *Agricultural and Forest Meteorology*, 149(11), 1800–1809. <https://doi.org/10.1016/j.agrformet.2009.06.009>
- Chiesi, M., Maselli, F., Bindi, M., Fibbi, L., Cherubini, P., Arlotta, E., Tirone, G., Matteucci, G., & Seufert, G. (2005). Modelling carbon budget of Mediterranean forests using ground and remote sensing measurements. *Agricultural and Forest Meteorology*, 135(1–4), 22–34. <https://doi.org/10.1016/j.agrformet.2005.09.011>
- Christensen, T. (2016). FLUXNET2015 SJ-Adv Adventdalen. <https://doi.org/10.18140/FLX/1440241>
- Chu, H., Baldocchi, D. D., Poindexter, C., Abraha, M., Desai, A. R., Bohrer, G., Arain, M. A., Griffis, T., Blanken, P. D., O'Halloran, T. L., Thomas, R. Q., Zhang, Q., Burns, S. P., Frank, J. M., Christian, D., Brown, S., Black, T. A., Gough, C. M., Law, B. E., ... Martin, T. A. (2018). Temporal Dynamics of Aerodynamic Canopy Height Derived From Eddy Covariance Mo-

- mentum Flux Data Across North American Flux Networks. *Geophysical Research Letters*, 45(17), 9275–9287. <https://doi.org/10.1029/2018gl079306>
- Chu, H., Chen, J., Gottgens, J. F., Desai, A. R., Ouyang, Z., & Qian, S. S. (2016). Response and biophysical regulation of carbon dioxide fluxes to climate variability and anomaly in contrasting ecosystems in northwestern Ohio, USA. *Agricultural and Forest Meteorology*, 220, 50–68. <https://doi.org/10.1016/j.agrformet.2016.01.008>
- Chu, H., Luo, X., Ouyang, Z., Chan, W. S., Dengel, S., Biraud, S. C., Torn, M. S., Metzger, S., Kumar, J., Arain, M. A., Arkebauer, T. J., Baldocchi, D., Bernacchi, C., Billesbach, D., Black, T. A., Blanken, P. D., Bohrer, G., Bracho, R., Brown, S., ... Zona, D. (2021). Representativeness of Eddy-Covariance flux footprints for areas surrounding AmeriFlux sites. *Agricultural and Forest Meteorology*, 301–302, 108350. <https://doi.org/10.1016/j.agrformet.2021.108350>
- Cleverly, J., Boulain, N., Villalobos-Vega, R., Grant, N., Faux, R., Wood, C., Cook, P. G., Yu, Q., Leigh, A., & Eamus, D. (2013). Dynamics of component carbon fluxes in a semi-arid acacia woodland, central Australia. *Journal of Geophysical Research: Biogeosciences*, 118(3), 1168–1185. <https://doi.org/10.1002/jgrg.20101>
- Cleverly, J., Boulain, N., Villalobos-Vega, R., Grant, N., Faux, R., Wood, C., Cook, P. G., Yu, Q., Leigh, A., & Eamus, D. (2013). Dynamics of component carbon fluxes in a semi-arid Acacia woodland, central Australia. *Journal of Geophysical Research: Biogeosciences*, 118(3), 1168–1185. <https://doi.org/10.1002/jgrg.20101>
- Cleverly, J., & Eamus, D. (2016a). FLUXNET2015 AU-ASM Alice Springs. <https://doi.org/10.18140/FLX/1440194>
- Cleverly, J., & Eamus, D. (2016b). FLUXNET2015 AU-TTE Ti Tree East. <https://doi.org/10.18140/FLX/1440205>
- Cremonese, E., Galvagno, M., Di Cella, U. M., & Migliavacca, M. (2016). FLUXNET2015 IT-Tor Torgnon. <https://doi.org/10.18140/FLX/1440237>
- De Ligne, A., Manise, T., Heinesch, B., Aubinet, M., & Vincke, C. (2016). FLUXNET2015 BE-Vie Vielsalm. <https://doi.org/10.18140/FLX/1440130>
- De Ligne, A., Manise, T., Moureaux, C., Aubinet, M., & Heinesch, B. (2016). FLUXNET2015 BE-Lon Lonzee. <https://doi.org/10.18140/FLX/1440129>
- Desai, A. (2016a). FLUXNET2015 US-Los Lost Creek. <https://doi.org/10.18140/FLX/1440076>
- Desai, A. (2016b). FLUXNET2015 US-PFa Park Falls/WLEF. <https://doi.org/10.18140/FLX/1440089>
- Desai, A. (2016c). FLUXNET2015 US-Syv Sylvania Wilderness Area. <https://doi.org/10.18140/FLX/1440091>

- Desai, A. (2016d). FLUXNET2015 US-WCr Willow Creek. <https://doi.org/10.18140/FLX/1440095>
- Desai, A. R., Noormets, A., Bolstad, P. V., Chen, J., Cook, B. D., Davis, K. J., Euskirchen, E. S., Gough, C., Martin, J. G., Ricciuto, D. M., Schmid, H. P., Tang, J., & Wang, W. (2008). Influence of vegetation and seasonal forcing on carbon dioxide fluxes across the Upper Midwest, USA: Implications for regional scaling. *Agricultural and Forest Meteorology*, 148(2), 288–308. <https://doi.org/10.1016/j.agrformet.2007.08.001>
- Dietiker, D., Buchmann, N., & Eugster, W. (2010). Testing the ability of the DNDC model to predict CO₂ and water vapour fluxes of a Swiss cropland site. *Agriculture, Ecosystems & Environment*, 139(3), 396–401. <https://doi.org/10.1016/j.agee.2010.09.002>
- Dolman, H., Hendriks, D., Parmentier, F.-J., Marchesini, L. B., Dean, J., & Van Huissteden, K. (2016). FLUXNET2015 NL-Hor Horstermeer. <https://doi.org/10.18140/FLX/1440177>
- Dolman, H., Van Der Molen, M., Parmentier, F.-J., Marchesini, L. B., Dean, J., Van Huissteden, K., & Maximov, T. (2016). FLUXNET2015 RU-Cok Chokurdakh. <https://doi.org/10.18140/FLX/1440182>
- Dong, G. (2016). FLUXNET2015 CN-Cng Changling. <https://doi.org/10.18140/FLX/1440209>
- Drake, B., & Hinkle, R. (2016a). FLUXNET2015 US-KS1 Kennedy Space Center (slash pine). <https://doi.org/10.18140/FLX/1440074>
- Drake, B., & Hinkle, R. (2016b). FLUXNET2015 US-KS2 Kennedy Space Center (scrub oak). <https://doi.org/10.18140/FLX/1440075>
- Dušek, J., Čížková, H., Stellner, S., Czerný, R., & Květ, J. (2012). Fluctuating water table affects gross ecosystem production and gross radiation use efficiency in a sedge-grass marsh. *Hydrobiologia*, 692(1), 57–66. <https://doi.org/10.1007/s10750-012-0998-z>
- Dušek, J., Janouš, D., & Pavelka, M. (2016). FLUXNET2015 CZ-wet Trebon (CZECHWET). <https://doi.org/10.18140/FLX/1440145>
- Elson, P., de Andrade, E. S., Lucas, G., May, R., Hattersley, R., Campbell, E., Dawson, A., Little, B., Raynaud, S., scmc72, Snow, A. D., Comer, R., Donkers, K., Blay, B., Killick, P., Wilson, N., Peglar, P., lgolston, lbdreyer, ... Havlin, C. (2023, August). SciTools/cartopy v0.22.0 on Github. <https://doi.org/10.5281/zenodo.1182735>
- Etzold, S., Ruehr, N. K., Zweifel, R., Dobbertin, M., Zingg, A., Pluess, P., Hässler, R., Eugster, W., & Buchmann, N. (2011). The Carbon Balance of Two Contrasting Mountain Forest Ecosystems in Switzerland: Similar Annual Trends, but Seasonal Differences. *Ecosystems*, 14(8), 1289–1309. <https://doi.org/10.1007/s10021-011-9481-3>
- Ewers, B., & Pendall, E. (2016). FLUXNET2015 US-Sta Saratoga. <https://doi.org/10.18140/FLX/1440115>

- Fares, S., Savi, F., Muller, J., Matteucci, G., & Paoletti, E. (2014). Simultaneous measurements of above and below canopy ozone fluxes help partitioning ozone deposition between its various sinks in a Mediterranean Oak Forest. *Agricultural and Forest Meteorology*, 198–199, 181–191. <https://doi.org/10.1016/j.agrformet.2014.08.014>
- Fares, S. (2016). FLUXNET2015 US-Lin Lindcove Orange Orchard. <https://doi.org/10.18140/FLX/1440107>
- Fares, S., Savi, F., & Conte, A. (2016). FLUXNET2015 IT-Cp2 Castelporziano 2. <https://doi.org/10.18140/FLX/1440233>
- Fares, S., Vargas, R., Detto, M., Goldstein, A. H., Karlik, J., Paoletti, E., & Vitale, M. (2013). Tropospheric ozone reduces carbon assimilation in trees: estimates from analysis of continuous flux measurements. *Global Change Biology*, 19(8), 2427–2443. <https://doi.org/10.1111/gcb.12222>
- Ferréa, C., Zenone, T., Comolli, R., & Seufert, G. (2012). Estimating heterotrophic and autotrophic soil respiration in a semi-natural forest of Lombardy, Italy. *Pedobiologia*, 55(6), 285–294. <https://doi.org/10.1016/j.pedobi.2012.05.001>
- Fischer, M. L., Torn, M. S., Billesbach, D. P., Doyle, G., Northup, B., & Biraud, S. C. (2012). Carbon, water, and heat flux responses to experimental burning and drought in a tallgrass prairie. *Agricultural and Forest Meteorology*, 166–167, 169–174. <https://doi.org/10.1016/j.agrformet.2012.07.011>
- FLUXNET.org. (2024). IGBP classification [<https://fluxnet.org/data/badm-data-templates/igbp-classification/>, last accessed: 08-Feb-2024].
- Friborg, T., Biasi, C., & Shurpali, N. J. (2016). FLUXNET2015 RU-Vrk Seida/Vorkuta. <https://doi.org/10.18140/FLX/1440245>
- Friborg, T., Jammet, M., & Crill, P. (2016). FLUXNET2015 SE-St1 Stordalen grassland. <https://doi.org/10.18140/FLX/1440187>
- Galvagno, M., Wohlfahrt, G., Cremonese, E., Rossini, M., Colombo, R., Filippa, G., Julitta, T., Manca, G., Siniscalco, C., Morra di Cellà, U., & Migliavacca, M. (2013). Phenology and carbon dioxide source/sink strength of a subalpine grassland in response to an exceptionally short snow season. *Environmental Research Letters*, 8(2), 025008. <https://doi.org/10.1088/1748-9326/8/2/025008>
- Garbulsky, M. F., Peñuelas, J., Papale, D., & Filella, I. (2008). Remote estimation of carbon dioxide uptake by a Mediterranean forest. *Global Change Biology*, 14(12), 2860–2867. <https://doi.org/10.1111/j.1365-2486.2008.01684.x>

- Garcia, A., Di Bella, C., Houspanossian, J., Magliano, P., Jobbág, E., Posse, G., Fernández, R., & Nosetto, M. (2016). FLUXNET2015 AR-SLu San Luis. <https://doi.org/10.18140/FLX/1440191>
- Gianelle, D., Cavagna, M., Zampedri, R., & Marcolla, B. (2016). FLUXNET2015 IT-MBo Monte Bondone. <https://doi.org/10.18140/FLX/1440170>
- Gianelle, D., Zampedri, R., Cavagna, M., & Sottocornola, M. (2016). FLUXNET2015 IT-Lav Lavarone. <https://doi.org/10.18140/FLX/1440169>
- Goldstein, A. (2016). FLUXNET2015 US-Blo Blodgett Forest. <https://doi.org/10.18140/FLX/1440068>
- Gough, C., Bohrer, G., & Curtis, P. (2016a). FLUXNET2015 US-UMB Univ. of Mich. Biological Station. <https://doi.org/10.18140/FLX/1440093>
- Gough, C., Bohrer, G., & Curtis, P. (2016b). FLUXNET2015 US-UMd UMBS Disturbance. <https://doi.org/10.18140/FLX/1440101>
- Goulden, M. (2016a). FLUXNET2015 BR-Sa3 Santarem-Km83-Logged Forest. <https://doi.org/10.18140/FLX/1440033>
- Goulden, M. (2016b). FLUXNET2015 CA-NS2 UCI-1930 burn site. <https://doi.org/10.18140/FLX/1440037>
- Goulden, M. (2016c). FLUXNET2015 CA-NS3 UCI-1964 burn site. <https://doi.org/10.18140/FLX/1440038>
- Goulden, M. (2016d). FLUXNET2015 CA-NS4 UCI-1964 burn site wet. <https://doi.org/10.18140/FLX/1440039>
- Goulden, M. (2016e). FLUXNET2015 CA-NS5 UCI-1981 burn site. <https://doi.org/10.18140/FLX/1440040>
- Goulden, M. (2016f). FLUXNET2015 CA-NS6 UCI-1989 burn site. <https://doi.org/10.18140/FLX/1440041>
- Goulden, M. (2016g). FLUXNET2015 CA-NS7 UCI-1998 burn site. <https://doi.org/10.18140/FLX/1440042>
- Gruening, C., Goded, I., Cescatti, A., Manca, G., & Seufert, G. (2016). FLUXNET2015 IT-SRo San Rossore. <https://doi.org/10.18140/FLX/1440176>
- Gruening, C., Goded, I., Cescatti, A., & Pokorska, O. (2016a). FLUXNET2015 IT-Isp Ispra ABC-IS. <https://doi.org/10.18140/FLX/1440234>
- Gruening, C., Goded, I., Cescatti, A., & Pokorska, O. (2016b). FLUXNET2015 IT-SR2 San Rossore 2. <https://doi.org/10.18140/FLX/1440236>

- Grünwald, T., & Bernhofer, C. (2007). A decade of carbon, water and energy flux measurements of an old spruce forest at the Anchor Station Tharandt. *Tellus B*, 59(3). <https://doi.org/10.3402/tellusb.v59i3.17000>
- Guan, D.-X., Wu, J.-B., Zhao, X.-S., Han, S.-J., Yu, G.-R., Sun, X.-M., & Jin, C.-J. (2006). CO₂ fluxes over an old, temperate mixed forest in northeastern China. *Agricultural and Forest Meteorology*, 137(3–4), 138–149. <https://doi.org/10.1016/j.agrformet.2006.02.003>
- Hansen, B. U. (2016). FLUXNET2015 GL-NuF Nuuk Fen. <https://doi.org/10.18140/FLX/1440222>
- Hodges, J. L. (1958). The significance probability of the smirnov two-sample test. *Arkiv för Matematik*, 3(5), 469–486. <https://doi.org/10.1007/bf02589501>
- Hommeltenberg, J., Schmid, H. P., Drösler, M., & Werle, P. (2014). Can a bog drained for forestry be a stronger carbon sink than a natural bog forest? *Biogeosciences*, 11(13), 3477–3493. <https://doi.org/10.5194/bg-11-3477-2014>
- Horn, J. E., & Schulz, K. (2011). Identification of a general light use efficiency model for gross primary production. *Biogeosciences*, 8(4), 999–1021. <https://doi.org/10.5194/bg-8-999-2011>
- Hörtnagl, L., Eugster, W., Buchmann, N., Paul-Limoges, E., Etzold, S., & Haeni, M. (2016). FLUXNET2015 CH-Lae Laegern. <https://doi.org/10.18140/FLX/1440134>
- Hörtnagl, L., Eugster, W., Merbold, L., Buchmann, N., Gharun, M., Etzold, S., Haesler, R., & Haeni, M. (2016). FLUXNET2015 CH-Dav Davos. <https://doi.org/10.18140/FLX/1440132>
- Hörtnagl, L., Feigenwinter, I., Fuchs, K., Merbold, L., Buchmann, N., Eugster, W., & Zeeman, M. (2016a). FLUXNET2015 CH-Cha Chamau. <https://doi.org/10.18140/FLX/1440131>
- Hörtnagl, L., Feigenwinter, I., Fuchs, K., Merbold, L., Buchmann, N., Eugster, W., & Zeeman, M. (2016b). FLUXNET2015 CH-Fru Früebüel. <https://doi.org/10.18140/FLX/1440133>
- Hörtnagl, L., Maier, R., Eugster, W., Buchmann, N., & Emmel, C. (2016). FLUXNET2015 CH-Oe2 Oensingen crop. <https://doi.org/10.18140/FLX/1440136>
- Hutley, L. B., Beringer, J., Isaac, P. R., Hacker, J. M., & Cernusak, L. A. (2011). A sub-continental scale living laboratory: Spatial patterns of savanna vegetation over a rainfall gradient in northern Australia. *Agricultural and Forest Meteorology*, 151(11), 1417–1428. <https://doi.org/10.1016/j.agrformet.2011.03.002>
- Ibrom, A., & Pilegaard, K. (2016). FLUXNET2015 DK-Sor Soroe. <https://doi.org/10.18140/FLX/1440155>
- Ikawa, H., Nakai, T., Busey, R. C., Kim, Y., Kobayashi, H., Nagai, S., Ueyama, M., Saito, K., Nagano, H., Suzuki, R., & Hinzman, L. (2015). Understory CO₂, sensible heat, and latent heat fluxes

- in a black spruce forest in interior Alaska. *Agricultural and Forest Meteorology*, 214–215, 80–90. <https://doi.org/10.1016/j.agrformet.2015.08.247>
- Imer, D., Merbold, L., Eugster, W., & Buchmann, N. (2013). Temporal and spatial variations of soil CO₂, CH₄ and N₂O fluxes at three differently managed grasslands. *Biogeosciences*, 10(9), 5931–5945. <https://doi.org/10.5194/bg-10-5931-2013>
- Jacobs, C. M. J., Jacobs, A. F. G., Bosveld, F. C., Hendriks, D. M. D., Hensen, A., Kroon, P. S., Moors, E. J., Nol, L., Schrier-Uijl, A., & Veenendaal, E. M. (2007). Variability of annual CO₂ exchange from Dutch grasslands. *Biogeosciences*, 4(5), 803–816. <https://doi.org/10.5194/bg-4-803-2007>
- Jammet, M., Crill, P., Dengel, S., & Friborg, T. (2015). Large methane emissions from a subarctic lake during spring thaw: Mechanisms and landscape significance. *Journal of Geophysical Research: Biogeosciences*, 120(11), 2289–2305. <https://doi.org/10.1002/2015jg003137>
- Kato, T., Tang, Y., Gu, S., Hirota, M., Du, M., Li, Y., & Zhao, X. (2006). Temperature and biomass influences on interannual changes in CO₂ exchange in an alpine meadow on the Qinghai-Tibetan Plateau. *Global Change Biology*, 12(7), 1285–1298. <https://doi.org/10.1111/j.1365-2486.2006.01153.x>
- Keppel-Aleks, G., Wennberg, P. O., Washenfelder, R. A., Wunch, D., Schneider, T., Toon, G. C., Andres, R. J., Blavier, J.-F., Connor, B., Davis, K. J., Desai, A. R., Messerschmidt, J., Notholt, J., Roehl, C. M., Sherlock, V., Stephens, B. B., Vay, S. A., & Wofsy, S. C. (2012). The imprint of surface fluxes and transport on variations in total column carbon dioxide. *Biogeosciences*, 9(3), 875–891. <https://doi.org/10.5194/bg-9-875-2012>
- Kilinc, M., Beringer, J., Hutley, L. B., Tapper, N. J., & McGuire, D. A. (2013). Carbon and water exchange of the world's tallest angiosperm forest. *Agricultural and Forest Meteorology*, 182–183, 215–224. <https://doi.org/10.1016/j.agrformet.2013.07.003>
- Klatt, J., Schmid, H. P., Mauder, M., & Steinbrecher, R. (2016). FLUXNET2015 DE-SfN Schechenfilz Nord. <https://doi.org/10.18140/FLX/1440219>
- Knöhl, A., Schulze, E.-D., Kolle, O., & Buchmann, N. (2003a). Large carbon uptake by an unmanaged 250-year-old deciduous forest in central Germany. *Agricultural and Forest Meteorology*, 118(3), 151–167. [https://doi.org/10.1016/S0168-1923\(03\)00115-1](https://doi.org/10.1016/S0168-1923(03)00115-1)
- Knöhl, A., Schulze, E.-D., Kolle, O., & Buchmann, N. (2003b). Large carbon uptake by an unmanaged 250-year-old deciduous forest in Central Germany. *Agricultural and Forest Meteorology*, 118(3–4), 151–167. [https://doi.org/10.1016/s0168-1923\(03\)00115-1](https://doi.org/10.1016/s0168-1923(03)00115-1)
- Knöhl, A., Tiedemann, F., Kolle, O., Schulze, E.-D., Anthoni, P., Kutsch, W., Herbst, M., & Siebicke, L. (2016). FLUXNET2015 DE-Lnf Leinefelde. <https://doi.org/10.18140/FLX/1440150>

- Knohl, A., Tiedemann, F., Kolle, O., Schulze, E.-D., Kutsch, W., Herbst, M., & Siebicke, L. (2016). FLUXNET2015 DE-Hai Hainich. <https://doi.org/10.18140/FLX/1440148>
- Kobayashi, H., & Suzuki, R. (2016). FLUXNET2015 US-Prr Poker Flat Research Range Black Spruce Forest. <https://doi.org/10.18140/FLX/1440113>
- Korkiakoski, M., Tuovinen, J.-P., Aurela, M., Koskinen, M., Minkkinen, K., Ojanen, P., Penttilä, T., Rainne, J., Laurila, T., & Lohila, A. (2017). Methane exchange at the peatland forest floor – automatic chamber system exposes the dynamics of small fluxes. *Biogeosciences*, 14(7), 1947–1967. <https://doi.org/10.5194/bg-14-1947-2017>
- Kotani, A. (2016a). FLUXNET2015 JP-MBF Moshiri Birch Forest Site. <https://doi.org/10.18140/FLX/1440238>
- Kotani, A. (2016b). FLUXNET2015 JP-SMF Seto Mixed Forest Site. <https://doi.org/10.18140/FLX/1440239>
- Kurbatova, J., Li, C., Varlagin, A., Xiao, X., & Vygodskaya, N. (2008). Modeling carbon dynamics in two adjacent spruce forests with different soil conditions in Russia. *Biogeosciences*, 5(4), 969–980. <https://doi.org/10.5194/bg-5-969-2008>
- Kurc, S. (2016). FLUXNET2015 US-SRC Santa Rita Creosote. <https://doi.org/10.18140/FLX/1440098>
- Kutsch, W. L., Merbold, L., & Kolle, O. (2016). FLUXNET2015 ZM-Mon Mongu. <https://doi.org/10.18140/FLX/1440189>
- Kutzbach, L., Sachs, T., Boike, J., Wille, C., Schreiber, P., Langer, M., & Pfeiffer, E.-M. (2016). FLUXNET2015 RU-Sam Samoylov. <https://doi.org/10.18140/FLX/1440185>
- Kwon, H.-J., Oechel, W. C., Zulueta, R. C., & Hastings, S. J. (2006). Effects of climate variability on carbon sequestration among adjacent wet sedge tundra and moist tussock tundra ecosystems. *Journal of Geophysical Research: Biogeosciences*, 111(G3). <https://doi.org/10.1029/2005jg000036>
- Law, B. (2016a). FLUXNET2015 US-Me1 Metolius - Eyerly burn. <https://doi.org/10.18140/FLX/1440078>
- Law, B. (2016b). FLUXNET2015 US-Me2 Metolius mature ponderosa pine. <https://doi.org/10.18140/FLX/1440079>
- Law, B. (2016c). FLUXNET2015 US-Me3 Metolius-second young aged pine. <https://doi.org/10.18140/FLX/1440080>
- Law, B. (2016d). FLUXNET2015 US-Me4 Metolius-old aged ponderosa pine. <https://doi.org/10.18140/FLX/1440081>

- Law, B. (2016e). FLUXNET2015 US-Me5 Metolius-first young aged pine. <https://doi.org/10.18140/FLX/1440082>
- Law, B. (2016f). FLUXNET2015 US-Me6 Metolius Young Pine Burn. <https://doi.org/10.18140/FLX/1440099>
- Leuning, R., Cleugh, H. A., Zegelin, S. J., & Hughes, D. (2005). Carbon and water fluxes over a temperate Eucalyptus forest and a tropical wet/dry savanna in Australia: measurements and comparison with MODIS remote sensing estimates. *Agricultural and Forest Meteorology*, 129(3–4), 151–173. <https://doi.org/10.1016/j.agrformet.2004.12.004>
- Liddell, M. J. (2016). FLUXNET2015 AU-Rob Robson Creek, Queensland, Australia. <https://doi.org/10.18140/FLX/1440203>
- Lindauer, M., Schmid, H., Grote, R., Mauder, M., Steinbrecher, R., & Wolpert, B. (2014). Net ecosystem exchange over a non-cleared wind-throw-disturbed upland spruce forest—Measurements and simulations. *Agricultural and Forest Meteorology*, 197, 219–234. <https://doi.org/10.1016/j.agrformet.2014.07.005>
- Lindauer, M., Steinbrecher, R., Wolpert, B., Mauder, M., & Schmid, H. P. (2016). FLUXNET2015 DE-Lkb Lackenberg. <https://doi.org/10.18140/FLX/1440214>
- Lohila, A., Aurela, M., Tuovinen, J.-P., Hatakka, J., & Laurila, T. (2016). FLUXNET2015 FI-Jok Jokioinen. <https://doi.org/10.18140/FLX/1440159>
- Lohila, A., Aurela, M., Tuovinen, J.-P., & Laurila, T. (2004). Annual CO₂ exchange of a peat field growing spring barley or perennial forage grass. *Journal of Geophysical Research: Atmospheres*, 109(D18). <https://doi.org/10.1029/2004jd004715>
- Lohila, A., Korkiakoski, M., Tuovinen, J.-P., Hatakka, J., Aurela, M., Rainne, J., Mäkelä, T., & Laurila, T. (2016). FLUXNET2015 FI-Let Lettosuo. <https://doi.org/10.18140/FLX/1440227>
- López-Ballesteros, A., Serrano-Ortiz, P., Kowalski, A. S., Sánchez-Cañete, E. P., Scott, R. L., & Domingo, F. (2017). Subterranean ventilation of allochthonous CO₂ governs net CO₂ exchange in a semiarid Mediterranean grassland. *Agricultural and Forest Meteorology*, 234–235, 115–126. <https://doi.org/10.1016/j.agrformet.2016.12.021>
- López-Blanco, E., Lund, M., Williams, M., Tamstorf, M. P., Westergaard-Nielsen, A., Exbrayat, J.-F., Hansen, B. U., & Christensen, T. R. (2017). Exchange of CO₂ in Arctic tundra: impacts of meteorological variations and biological disturbance. *Biogeosciences*, 14(19), 4467–4483. <https://doi.org/10.5194/bg-14-4467-2017>
- Loubet, B., Laville, P., Lehuger, S., Larmanou, E., Fléchard, C., Mascher, N., Genermont, S., Roche, R., Ferrara, R. M., Stella, P., Personne, E., Durand, B., Decuq, C., Flura, D., Masson, S., Fanucci, O., Rampon, J.-N., Siemens, J., Kindler, R., ... Cellier, P. (2011). Carbon, nitrogen

- and Greenhouse gases budgets over a four years crop rotation in northern France. *Plant and Soil*, 343(1–2), 109–137. <https://doi.org/10.1007/s11104-011-0751-9>
- Lüers, J., Westermann, S., Piel, K., & Boike, J. (2014). Annual CO₂ budget and seasonal CO₂ exchange signals at a high Arctic permafrost site on Spitsbergen, Svalbard archipelago. *Bio-geosciences*, 11(22), 6307–6322. <https://doi.org/10.5194/bg-11-6307-2014>
- Lund, M., Falk, J. M., Friberg, T., Mbufong, H. N., Sigsgaard, C., Soegaard, H., & Tamstorf, M. P. (2012). Trends in CO₂ exchange in a high Arctic tundra heath, 2000–2010. *Journal of Geophysical Research: Biogeosciences*, 117(G2). <https://doi.org/10.1029/2011jg001901>
- Lund, M., Jackowicz-Korczyński, M., & Abermann, J. (2016a). FLUXNET2015 GL-ZaF Zackenberg Fen. <https://doi.org/10.18140/FLX/1440223>
- Lund, M., Jackowicz-Korczyński, M., & Abermann, J. (2016b). FLUXNET2015 GL-ZaH Zackenberg Heath. <https://doi.org/10.18140/FLX/1440224>
- Macfarlane, C., Lambert, P., Byrne, J., Johnstone, C., & Smart, N. (2016). FLUXNET2015 AU-Gin Gingin. <https://doi.org/10.18140/FLX/1440199>
- Magliulo, V., Di Tommasi, P., Famulari, D., Gasbarra, D., Vitale, L., & Manco, A. (2016). FLUXNET2015 IT-BCi Borgo Cioffi. <https://doi.org/10.18140/FLX/1440166>
- Mammarella, I., Vesala, T., Keronen, P., Kolari, P., Launiainen, S., Pumpanen, J., Rannik, Ü., Siivola, E., Levula, J., & Pohja, T. (2016). FLUXNET2015 FI-Hyy Hyttiala. <https://doi.org/10.18140/FLX/1440158>
- Manca, G., & Goded, I. (2016). FLUXNET2015 IT-PT1 Parco Ticino forest. <https://doi.org/10.18140/FLX/1440172>
- Marcolla, B., Pitacco, A., & Cescatti, A. (2003). Canopy Architecture and Turbulence Structure in a Coniferous Forest. *Boundary-Layer Meteorology*, 108(1), 39–59. <https://doi.org/10.1023/a:1023027709805>
- Marcolla, B., Cescatti, A., Manca, G., Zorer, R., Cavagna, M., Fiora, A., Gianelle, D., Rodeghiero, M., Sottocornola, M., & Zampedri, R. (2011). Climatic controls and ecosystem responses drive the inter-annual variability of the net ecosystem exchange of an alpine meadow. *Agricultural and Forest Meteorology*, 151(9), 1233–1243. <https://doi.org/10.1016/j.agrformet.2011.04.015>
- Margolis, H. A. (2016). FLUXNET2015 CA-Qfo Quebec - Eastern Boreal, Mature Black Spruce. <https://doi.org/10.18140/FLX/1440045>
- Marras, S., Pyles, R., Sirca, C., Paw U, K., Snyder, R., Duce, P., & Spano, D. (2011). Evaluation of the Advanced Canopy–Atmosphere–Soil Algorithm (ACASA) model performance over

- Mediterranean maquis ecosystem. *Agricultural and Forest Meteorology*, 151(6), 730–745. <https://doi.org/10.1016/j.agrformet.2011.02.004>
- Massman, B. (2016a). FLUXNET2015 US-GBT GLEES Brooklyn Tower. <https://doi.org/10.18140/FLX/1440118>
- Massman, B. (2016b). FLUXNET2015 US-GLE GLEES. <https://doi.org/10.18140/FLX/1440069>
- Matamala, R. (2016). FLUXNET2015 US-IB2 Fermi National Accelerator Laboratory- Batavia (Prairie site). <https://doi.org/10.18140/FLX/1440072>
- Matsumoto, K., Ohta, T., Nakai, T., Kuwada, T., Daikoku, K., Iida, S., Yabuki, H., Kononov, A. V., van der Molen, M. K., Kodama, Y., Maximov, T. C., Dolman, A. J., & Hattori, S. (2008). Energy consumption and evapotranspiration at several boreal and temperate forests in the Far East. *Agricultural and Forest Meteorology*, 148(12), 1978–1989. <https://doi.org/10.1016/j.agrformet.2008.09.008>
- Matteucci, G. (2016). FLUXNET2015 IT-Col Collelongo. <https://doi.org/10.18140/FLX/1440167>
- Maximov, T. (2016). FLUXNET2015 RU-SkP Yakutsk Spasskaya Pad larch. <https://doi.org/10.18140/FLX/1440243>
- McCaughey, H. (2016). FLUXNET2015 CA-Gro Ontario - Groundhog River, Boreal Mixedwood Forest. <https://doi.org/10.18140/FLX/1440034>
- McEwing, K. R., Fisher, J. P., & Zona, D. (2015). Environmental and vegetation controls on the spatial variability of CH₄ emission from wet-sedge and tussock tundra ecosystems in the Arctic. *Plant and Soil*, 388(1–2), 37–52. <https://doi.org/10.1007/s11104-014-2377-1>
- McHugh, I. D., Beringer, J., Cunningham, S. C., Baker, P. J., Cavagnaro, T. R., Mac Nally, R., & Thompson, R. M. (2017). Interactions between nocturnal turbulent flux, storage and advection at an “ideal” eucalypt woodland site. *Biogeosciences*, 14(12), 3027–3050. <https://doi.org/10.5194/bg-14-3027-2017>
- Mengoli, G., Agustí-Panareda, A., Boussetta, S., Harrison, S. P., Trotta, C., & Prentice, I. C. (2022). Ecosystem photosynthesis in land-surface models: A first-principles approach incorporating acclimation. *Journal of Advances in Modeling Earth Systems*, 14(1). <https://doi.org/10.1029/2021MS002767>
- Merbold, L., Ardö, J., Arneth, A., Scholes, R. J., Nouvellon, Y., de Grandcourt, A., Archibald, S., Bonnefond, J. M., Boulain, N., Brueggemann, N., Bruemmer, C., Cappelaere, B., Ceschia, E., El-Khidir, H. A. M., El-Tahir, B. A., Falk, U., Lloyd, J., Kergoat, L., Le Dantec, V., ... Kutsch, W. L. (2009). Precipitation as driver of carbon fluxes in 11 African ecosystems. *Biogeosciences*, 6(6), 1027–1041. <https://doi.org/10.5194/bg-6-1027-2009>

- Merbold, L., Kutsch, W. L., Corradi, C., Kolle, O., Rebmann, C., Stoy, P. C., Zimov, S. A., & Schulze, E.-D. (2009). Artificial drainage and associated carbon fluxes (CO_2/CH_4) in a tundra ecosystem. *Global Change Biology*, 15(11), 2599–2614. <https://doi.org/10.1111/j.1365-2486.2009.01962.x>
- Merbold, L., Eugster, W., Stieger, J., Zahniser, M., Nelson, D., & Buchmann, N. (2014). Greenhouse gas budget (CO_2 , CH_4 and N_2O) of intensively managed grassland following restoration. *Global Change Biology*, 20(6), 1913–1928. <https://doi.org/10.1111/gcb.12518>
- Merbold, L., Rebmann, C., & Corradi, C. (2016). FLUXNET2015 RU-Che Cherski. <https://doi.org/10.18140/FLX/1440181>
- Meyer, W. S., Kondrlovà, E., & Koerber, G. R. (2015). Evaporation of perennial semi-arid woodland in southeastern Australia is adapted for irregular but common dry periods. *Hydrological Processes*, 29(17), 3714–3726. <https://doi.org/10.1002/hyp.10467>
- Meyer, W., Cale, P., Koerber, G., Ewenz, C., & Sun, Q. (2016). FLUXNET2015 AU-Cpr Calperum. <https://doi.org/10.18140/FLX/1440195>
- Meyers, T. (2016). FLUXNET2015 US-Goo Goodwin Creek. <https://doi.org/10.18140/FLX/1440070>
- Migliavacca, M., Meroni, M., Busetto, L., Colombo, R., Zenone, T., Matteucci, G., Manca, G., & Seufert, G. (2009). Modeling Gross Primary Production of Agro-Forestry Ecosystems by Assimilation of Satellite-Derived Information in a Process-Based Model. *Sensors*, 9(2), 922–942. <https://doi.org/10.3390/s90200922>
- Montagnani, L., Manca, G., Canepa, E., Georgieva, E., Acosta, M., Feigenwinter, C., Janous, D., Kerschbaumer, G., Lindroth, A., Minach, L., Minerbi, S., Mölder, M., Pavelka, M., Seufert, G., Zeri, M., & Ziegler, W. (2009). A new mass conservation approach to the study of CO_2 advection in an alpine forest. *Journal of Geophysical Research: Atmospheres*, 114(D7). <https://doi.org/10.1029/2008jd010650>
- Montagnani, L., & Minerbi, S. (2016). FLUXNET2015 IT-Ren Renon. <https://doi.org/10.18140/FLX/1440173>
- Moors, E. J. (2012). *Water use of forests in the Netherlands* [PhD thesis]. Vrije Universiteit Amsterdam. Alterra scientific contributions: 41. <https://edepot.wur.nl/213926>
- Moors, E., & Elbers, J. (2016). FLUXNET2015 NL-Loo Loobos. <https://doi.org/10.18140/FLX/1440178>
- Moureaux, C., Debacq, A., Bodson, B., Heinesch, B., & Aubinet, M. (2006). Annual net ecosystem carbon exchange by a sugar beet crop. *Agricultural and Forest Meteorology*, 139(1–2), 25–39. <https://doi.org/10.1016/j.agrformet.2006.05.009>

- Munger, J. W. (2016). FLUXNET2015 US-Ha1 Harvard Forest EMS Tower (HFR1). <https://doi.org/10.18140/FLX/1440071>
- Neirynck, J., Verbeeck, H., Carrara, A., Kowalski, A. S., Ceulemans, R., Janssens, I. A., Gielen, B., & Roland, M. (2016). FLUXNET2015 BE-Bra Brasschaat. <https://doi.org/10.18140/FLX/1440128>
- Novick, K., & Phillips, R. (2016). FLUXNET2015 US-MMS Morgan Monroe State Forest. <https://doi.org/10.18140/FLX/1440083>
- Olesen, J. (2016). FLUXNET2015 DK-Fou Foulum. <https://doi.org/10.18140/FLX/1440154>
- Ourcival, J.-M. (2016). FLUXNET2015 FR-Pue Puechabon. <https://doi.org/10.18140/FLX/1440164>
- Papale, D., Tirone, G., Valentini, R., Arriga, N., Belelli, L., Consalvo, C., Dore, S., Manca, G., Mazzenga, F., Sabbatini, S., & Stefani, P. (2016). FLUXNET2015 IT-Ro2 Roccarespampani 2. <https://doi.org/10.18140/FLX/1440175>
- Pastorello, G., Trotta, C., Canfora, E., Chu, H., Christianson, D., Cheah, Y.-W., Poindexter, C., Chen, J., Elbashandy, A., Humphrey, M., et al. (2020). The FLUXNET2015 dataset and the ONEFlux processing pipeline for eddy covariance data. *Scientific Data*, 7(1), 225. <https://doi.org/10.1038/s41597-020-0534-3>
- Pendall, E., & Griebel, A. (2016). FLUXNET2015 AU-Cum Cumberland Plains. <https://doi.org/10.18140/FLX/1440196>
- Pilegaard, K., & Ibrom, A. (2016). FLUXNET2015 DK-Eng Enghave. <https://doi.org/10.18140/FLX/1440153>
- Pilegaard, K., Ibrom, A., Courtney, M. S., Hummelshøj, P., & Jensen, N. O. (2011). Increasing net CO₂ uptake by a Danish beech forest during the period from 1996 to 2009. *Agricultural and Forest Meteorology*, 151(7), 934–946. <https://doi.org/10.1016/j.agrformet.2011.02.013>
- Posse, G., Lewczuk, N., Richter, K., & Cristiano, P. (2016a). Carbon and water vapor balance in a subtropical pine plantation. *iForest - Biogeosciences and Forestry*, 9(5), 736–742. <https://doi.org/10.3832/ifor1815-009>
- Posse, G., Lewczuk, N., Richter, K., & Cristiano, P. (2016b). FLUXNET2015 AR-Vir Virasoro. <https://doi.org/10.18140/FLX/1440192>
- Poveda, F. D., Ballesteros, A. L., Cañete, E. P. S., Ortiz, P. S., Jiménez, M. R. M., Priego, O. P., & Kowalski, A. S. (2016). FLUXNET2015 ES-Amo Amoladeras. <https://doi.org/10.18140/FLX/1440156>

- Prescher, A.-K., Grünwald, T., & Bernhofer, C. (2010). Land use regulates carbon budgets in eastern Germany: From NEE to NBP. *Agricultural and Forest Meteorology*, 150(7–8), 1016–1025. <https://doi.org/10.1016/j.agrformet.2010.03.008>
- Rambal, S., Joffre, R., Ourcival, J. M., Cavender-Bares, J., & Rocheteau, A. (2004). The growth respiration component in eddy CO₂ flux from a Quercus ilex mediterranean forest. *Global Change Biology*, 10(9), 1460–1469. <https://doi.org/10.1111/j.1365-2486.2004.00819.x>
- Reed, D. E., Ewers, B. E., Pendall, E., Naithani, K. J., Kwon, H., & Kelly, R. D. (2018). Biophysical Factors and Canopy Coupling Control Ecosystem Water and Carbon Fluxes of Semiarid Sagebrush Ecosystems. *Rangeland Ecology & Management*, 71(3), 309–317. <https://doi.org/10.1016/j.rama.2018.01.003>
- Reverter, B. R., Sánchez-Cañete, E. P., Resco, V., Serrano-Ortiz, P., Oyonarte, C., & Kowalski, A. S. (2010). Analyzing the major drivers of NEE in a Mediterranean alpine shrubland. *Biogeosciences*, 7(9), 2601–2611. <https://doi.org/10.5194/bg-7-2601-2010>
- Reverter, B. R., Perez-Cañete, E. S., & Kowalski, A. S. (2016a). FLUXNET2015 ES-LgS Laguna Seca. <https://doi.org/10.18140/FLX/1440225>
- Reverter, B. R., Perez-Cañete, E. S., & Kowalski, A. S. (2016b). FLUXNET2015 ES-Ln2 Lanjaron-Salvage logging. <https://doi.org/10.18140/FLX/1440226>
- Rey, A., Pegoraro, E., Tedeschi, V., De Parri, I., Jarvis, P. G., & Valentini, R. (2002). Annual variation in soil respiration and its components in a coppice oak forest in Central Italy. *Global Change Biology*, 8(9), 851–866. <https://doi.org/10.1046/j.1365-2486.2002.00521.x>
- Rubel, F., Brugger, K., Haslinger, K., & Auer, I. (2017). The climate of the european alps: Shift of very high resolution Köppen-Geiger climate zones 1800 – 2100. *Meteorologische Zeitschrift*, 26(2), 115–125. <https://doi.org/10.1127/metz/2016/0816>
- Runkle, B. R. K., Rigby, J. R., Reba, M. L., Anapalli, S. S., Bhattacharjee, J., Krauss, K. W., Liang, L., Locke, M. A., Novick, K. A., Sui, R., Suvočarev, K., & White, P. M. (2017). Delta-Flux: An Eddy Covariance Network for a Climate-Smart Lower Mississippi Basin. *Agricultural & Environmental Letters*, 2(1). <https://doi.org/10.2134/ael2017.01.0003>
- Sabbatini, S., Arriga, N., Bertolini, T., Castaldi, S., Chiti, T., Consalvo, C., Njakou Djomo, S., Gioli, B., Matteucci, G., & Papale, D. (2016). Greenhouse gas balance of cropland conversion to bioenergy poplar short-rotation coppice. *Biogeosciences*, 13(1), 95–113. <https://doi.org/10.5194/bg-13-95-2016>
- Sabbatini, S., Arriga, N., Gioli, B., & Papale, D. (2016). FLUXNET2015 IT-CA2 Castel d'Asso2. <https://doi.org/10.18140/FLX/1440231>

- Sabbatini, S., Arriga, N., Matteucci, G., & Papale, D. (2016). FLUXNET2015 IT-CA3 Castel d'Asso 3. <https://doi.org/10.18140/FLX/1440232>
- Sabbatini, S., Arriga, N., & Papale, D. (2016). FLUXNET2015 IT-CA1 Castel d'Asso1. <https://doi.org/10.18140/FLX/1440230>
- Sachs, T., Wille, C., Larmanou, E., & Franz, D. (2016). FLUXNET2015 DE-Zrk Zarnekow. <https://doi.org/10.18140/FLX/1440221>
- Saleska, S. (2016). FLUXNET2015 BR-Sa1 Santarem-Km67-Primary Forest. <https://doi.org/10.18140/FLX/1440032>
- Sanchez, C. R., Sturtevant, C., Szutu, D., Baldocchi, D., Eichelmann, E., & Knox, S. (2016). FLUXNET2015 US-Tw4 Twitchell East End Wetland. <https://doi.org/10.18140/FLX/1440111>
- Schmidt, M., Reichenau, T., Fiener, P., & Schneider, K. (2012). The carbon budget of a winter wheat field: An eddy covariance analysis of seasonal and inter-annual variability. *Agricultural and Forest Meteorology*, 165, 114–126. <https://doi.org/10.1016/j.agrformet.2012.05.012>
- Schneider, K., & Schmidt, M. (2016). FLUXNET2015 DE-Seh Selhausen. <https://doi.org/10.18140/FLX/1440217>
- Scholes, B. (2016). FLUXNET2015 ZA-Kru Skukuza. <https://doi.org/10.18140/FLX/1440188>
- Schroder, I. (2014). Arcturus Emerald OzFlux tower site OzFlux: Australian and New Zealand flux research and monitoring [hdl: 102.100.100/14249]. <https://doi.org/102.100.100/14249>
- Schroder, I., Zegelin, S., Palu, T., & Feitz, A. (2016). FLUXNET2015 AU-Emr Emerald. <https://doi.org/10.18140/FLX/1440198>
- Scott, R. (2016a). FLUXNET2015 US-Whs Walnut Gulch Lucky Hills Shrub. <https://doi.org/10.18140/FLX/1440097>
- Scott, R. (2016b). FLUXNET2015 US-SRG Santa Rita Grassland. <https://doi.org/10.18140/FLX/1440114>
- Scott, R. (2016c). FLUXNET2015 US-SRM Santa Rita Mesquite. <https://doi.org/10.18140/FLX/1440090>
- Scott, R. (2016d). FLUXNET2015 US-Wkg Walnut Gulch Kendall Grasslands. <https://doi.org/10.18140/FLX/1440096>
- Serrano-Ortiz, P., Domingo, F., Cazorla, A., Were, A., Cuevva, S., Villagarcía, L., Alados-Arboledas, L., & Kowalski, A. S. (2009). Interannual CO₂ exchange of a sparse Mediterranean shrubland on a carbonaceous substrate. *Journal of Geophysical Research: Biogeosciences*, 114(G4). <https://doi.org/10.1029/2009jg000983>

- Shao, C. (2016a). FLUXNET2015 CN-Du3 Duolun Degraded Meadow. <https://doi.org/10.18140/FLX/1440210>
- Shao, C. (2016b). FLUXNET2015 CN-Sw2 Siziwang Grazed (SZWG). <https://doi.org/10.18140/FLX/1440212>
- Shi, P., Sun, X., Xu, L., Zhang, X., He, Y., Zhang, D., & Yu, G. (2006). Net ecosystem CO₂ exchange and controlling factors in a steppe—Kobresia meadow on the Tibetan Plateau. *Science in China Series D: Earth Sciences*, 49(S2), 207–218. <https://doi.org/10.1007/s11430-006-8207-4>
- Shi, P., Zhang, X., & He, Y. (2016). FLUXNET2015 CN-Dan Dangxiong. <https://doi.org/10.18140/FLX/1440138>
- Sigut, L., Havrankova, K., Jocher, G., Pavelka, M., & Janouš, D. (2016a). FLUXNET2015 CZ-BK1 Bily Kriz forest. <https://doi.org/10.18140/FLX/1440143>
- Sigut, L., Havrankova, K., Jocher, G., Pavelka, M., & Janouš, D. (2016b). FLUXNET2015 CZ-BK2 Bily Kriz grassland. <https://doi.org/10.18140/FLX/1440144>
- Soegaard, H. (1999). Carbon dioxide exchange in a high-arctic fen estimated by eddy covariance measurements and modelling. *Global Change Biology*, 5(5), 547. <https://doi.org/10.1046/j.1365-2486.1999.00250.x>
- Spano, D., Duce, P., Marras, S., Sirca, C., Arca, A., Zara, P., & Ventura, A. (2016). FLUXNET2015 IT-Noe Arca di Noe - Le Prigionette. <https://doi.org/10.18140/FLX/1440171>
- Stocker, B. D., & Hufkens, K. (2021, May). geco-bern/rpmodel on Github. <https://doi.org/10.5281/zenodo.3359706>
- Stocker, B. D., Wang, H., Smith, N. G., Harrison, S. P., Keenan, T. F., Sandoval, D., Davis, T., & Prentice, I. C. (2020). P-model v1.0: An optimality-based light use efficiency model for simulating ecosystem gross primary production. *Geoscientific Model Development*, 13(3), 1545–1581. <https://doi.org/10.5194/gmd-13-1545-2020>
- Sturtevant, C., Szutu, D., Baldocchi, D., Matthes, J. H., Oikawa, P., & Chamberlain, S. D. (2016). FLUXNET2015 US-Myb Mayberry Wetland. <https://doi.org/10.18140/FLX/1440105>
- Sullivan, R. C., Cook, D. R., Ghate, V. P., Kotamarthi, V. R., & Feng, Y. (2019). Improved Spatiotemporal Representativeness and Bias Reduction of Satellite-Based Evapotranspiration Retrievals via Use of In Situ Meteorology and Constrained Canopy Surface Resistance. *Journal of Geophysical Research: Biogeosciences*, 124(2), 342–352. <https://doi.org/10.1029/2018jg004744>
- Suni, T., Rinne, J., Reissell, A., Altimir, N., Keronen, P., Rannik, U., Dal Maso, M., Kulmala, M., & Vesala, T. (2003). Long-term measurements of surface fluxes above a scots pine forest in

- hyytiala, southern finland, 1996-2001. *Boreal Environment Research*, 8(4), 287–301. <https://www.borenv.net/BER/archive/pdfs/ber8/ber8-287.pdf>
- Suyker, A. (2016a). FLUXNET2015 US-Ne1 Mead - irrigated continuous maize site. <https://doi.org/10.18140/FLX/1440084>
- Suyker, A. (2016b). FLUXNET2015 US-Ne2 Mead - irrigated maize-soybean rotation site. <https://doi.org/10.18140/FLX/1440085>
- Suyker, A. (2016c). FLUXNET2015 US-Ne3 Mead - rainfed maize-soybean rotation site. <https://doi.org/10.18140/FLX/1440086>
- Szutu, D., & Baldocchi, D. (2016). FLUXNET2015 US-Tw3 Twitchell Alfalfa. <https://doi.org/10.18140/FLX/1440110>
- Szutu, D., Baldocchi, D., Eichelmann, E., & Knox, S. (2016). FLUXNET2015 US-Tw1 Twitchell Wetland West Pond. <https://doi.org/10.18140/FLX/1440108>
- Tagesson, T., Ardö, J., & Fensholt, R. (2016). FLUXNET2015 SN-Dhr Dahra. <https://doi.org/10.18140/FLX/1440246>
- Tagesson, T., Fensholt, R., Guiro, I., Rasmussen, M. O., Huber, S., Mbow, C., Garcia, M., Horion, S., Sandholt, I., Holm-Rasmussen, B., Götsche, F. M., Ridler, M.-E., Olén, N., Lundegard Olsen, J., Ehammer, A., Madsen, M., Olesen, F. S., & Ardö, J. (2014). Ecosystem properties of semiarid savanna grassland in West Africa and its relationship with environmental variability. *Global Change Biology*, 21(1), 250–264. <https://doi.org/10.1111/gcb.12734>
- Tamrakar, R., Rayment, M. B., Moyano, F., Mund, M., & Knohl, A. (2018). Implications of structural diversity for seasonal and annual carbon dioxide fluxes in two temperate deciduous forests. *Agricultural and Forest Meteorology*, 263, 465–476. <https://doi.org/10.1016/j.agrformet.2018.08.027>
- Tang, Y., Kato, T., & Du, M. (2016). FLUXNET2015 CN-HaM Haibei Alpine Tibet site. <https://doi.org/10.18140/FLX/1440190>
- Tedeschi, V., Rey, A., Manca, G., Valentini, R., Jarvis, P. G., & Borghetti, M. (2005). Soil respiration in a Mediterranean oak forest at different developmental stages after coppicing. *Global Change Biology*, 12(1), 110–121. <https://doi.org/10.1111/j.1365-2486.2005.01081.x>
- Thum, T., Aalto, T., Laurila, T., Aurela, M., Kolari, P., & Hari, P. (2007). Parametrization of two photosynthesis models at the canopy scale in a northern boreal Scots pine forest. *Tellus B*, 59(5). <https://doi.org/10.3402/tellusb.v59i5.17066>
- Torn, M. (2016a). FLUXNET2015 US-ARb ARM Southern Great Plains burn site- Lamont. <https://doi.org/10.18140/FLX/1440064>

- Torn, M. (2016b). FLUXNET2015 US-ARc ARM Southern Great Plains control site- Lamont. <https://doi.org/10.18140/FLX/1440065>
- Tramontana, G., Jung, M., Schwalm, C. R., Ichii, K., Camps-Valls, G., Ráduly, B., Reichstein, M., Arain, M. A., Cescatti, A., Kiely, G., Merbold, L., Serrano-Ortiz, P., Sickert, S., Wolf, S., & Papale, D. (2016). Predicting carbon dioxide and energy fluxes across global fluxnet sites with regression algorithms. *Biogeosciences*, 13(14), 4291–4313. <https://doi.org/10.5194/bg-13-4291-2016>
- Trautmann, T., Koirala, S., Carvalhais, N., Eicker, A., Fink, M., Niemann, C., & Jung, M. (2018). Understanding terrestrial water storage variations in northern latitudes across scales. *Hydrology and Earth System Sciences*, 22(7), 4061–4082. <https://doi.org/10.5194/hess-22-4061-2018>
- Ulke, A. G., Gattinoni, N. N., & Posse, G. (2015). Analysis and modelling of turbulent fluxes in two different ecosystems in Argentina. *International Journal of Environment and Pollution*, 58(1/2), 52. <https://doi.org/10.1504/ijep.2015.076583>
- Valentini, R., De Angelis, P., Matteucci, G., Monaco, R., Dore, S., & Mucnozza, G. E. S. (1996). Seasonal net carbon dioxide exchange of a beech forest with the atmosphere. *Global Change Biology*, 2(3), 199–207. <https://doi.org/10.1111/j.1365-2486.1996.tb00072.x>
- Valentini, R., Dore, S., Mazzenga, F., Sabbatini, S., Stefani, P., Tirone, G., & Papale, D. (2016). FLUXNET2015 IT-Cpz Castelporziano. <https://doi.org/10.18140/FLX/1440168>
- Valentini, R., Tirone, G., Vitale, D., Papale, D., Arriga, N., Belelli, L., Dore, S., Manca, G., Mazzenga, F., Pegoraro, E., Sabbatini, S., & Stefani, P. (2016). FLUXNET2015 IT-Ro1 Roccarespani 1. <https://doi.org/10.18140/FLX/1440174>
- Van der Molen, M. K., van Huissteden, J., Parmentier, F. J. W., Petrescu, A. M. R., Dolman, A. J., Maximov, T. C., Kononov, A. V., Karsanaev, S. V., & Suzdalov, D. A. (2007). The growing season greenhouse gas balance of a continental tundra site in the Indigirka lowlands, NE Siberia. *Biogeosciences*, 4(6), 985–1003. <https://doi.org/10.5194/bg-4-985-2007>
- Varlagin, A., Kurbatova, J., & Vygodskaya, N. (2016). FLUXNET2015 RU-Fyo Fyodorovskoye. <https://doi.org/10.18140/FLX/1440183>
- Vitale, L., Di Tommasi, P., D'Urso, G., & Magliulo, V. (2015). The response of ecosystem carbon fluxes to LAI and environmental drivers in a maize crop grown in two contrasting seasons. *International Journal of Biometeorology*, 60(3), 411–420. <https://doi.org/10.1007/s00484-015-1038-2>
- Wang, H., & Fu, X. (2016). FLUXNET2015 CN-Qia Qianyanzhou. <https://doi.org/10.18140/FLX/1440141>

- Wohlfahrt, G., Hammerle, A., Haslwanter, A., Bahn, M., Tappeiner, U., & Cernusca, A. (2008). Seasonal and inter-annual variability of the net ecosystem CO₂ exchange of a temperate mountain grassland: Effects of weather and management. *Journal of Geophysical Research: Atmospheres*, 113(D8). <https://doi.org/10.1029/2007jd009286>
- Wohlfahrt, G., Hammerle, A., & Hörtnagl, L. (2016). FLUXNET2015 AT-Neu Neustift. <https://doi.org/10.18140/FLX/1440121>
- Wolf, S., Eugster, W., & Buchmann, N. (2016a). FLUXNET2015 PA-SPn Sardinilla Plantation. <https://doi.org/10.18140/FLX/1440180>
- Wolf, S., Eugster, W., & Buchmann, N. (2016b). FLUXNET2015 PA-SPs Sardinilla-Pasture. <https://doi.org/10.18140/FLX/1440179>
- Wolf, S., Eugster, W., Potvin, C., Turner, B. L., & Buchmann, N. (2011). Carbon sequestration potential of tropical pasture compared with afforestation in Panama. *Global Change Biology*, 17(9), 2763–2780. <https://doi.org/10.1111/j.1365-2486.2011.02460.x>
- Wolf, S., Keenan, T. F., Fisher, J. B., Baldocchi, D. D., Desai, A. R., Richardson, A. D., Scott, R. L., Law, B. E., Litvak, M. E., Brunsell, N. A., Peters, W., & van der Laan-Luijkx, I. T. (2016). Warm spring reduced carbon cycle impact of the 2012 US summer drought. *Proceedings of the National Academy of Sciences*, 113(21), 5880–5885. <https://doi.org/10.1073/pnas.1519620113>
- Woodgate, W., Van Gorsel, E., & Leuning, R. (2016). FLUXNET2015 AU-Tum Tumbarumba. <https://doi.org/10.18140/FLX/1440126>
- Yee, M. S., Pauwels, V. R., Daly, E., Beringer, J., Rüdiger, C., McCabe, M. F., & Walker, J. P. (2015). A comparison of optical and microwave scintillometers with eddy covariance derived surface heat fluxes. *Agricultural and Forest Meteorology*, 213, 226–239. <https://doi.org/10.1016/j.agrformet.2015.07.004>
- Yu, G.-R., Wen, X.-F., Sun, X.-M., Tanner, B. D., Lee, X., & Chen, J.-Y. (2006). Overview of ChinaFLUX and evaluation of its eddy covariance measurement. *Agricultural and Forest Meteorology*, 137(3–4), 125–137. <https://doi.org/10.1016/j.agrformet.2006.02.011>
- Zak, D., Reuter, H., Augustin, J., Shatwell, T., Barth, M., Gelbrecht, J., & McInnes, R. J. (2015). Changes of the CO₂ and CH₄ production potential of rewetted fens in the perspective of temporal vegetation shifts. *Biogeosciences*, 12(8), 2455–2468. <https://doi.org/10.5194/bg-12-2455-2015>
- Zhang, J., & Han, S. (2016). FLUXNET2015 CN-Cha Changbaishan. <https://doi.org/10.18140/FLX/1440137>

- Zhou, G., & Yan, J. (2016). FLUXNET2015 CN-Din Dinghushan. <https://doi.org/10.18140/FLX/1440139>
- Zielis, S., Etzold, S., Zweifel, R., Eugster, W., Haeni, M., & Buchmann, N. (2014). NEP of a Swiss subalpine forest is significantly driven not only by current but also by previous year's weather. *Biogeosciences*, 11(6), 1627–1635. <https://doi.org/10.5194/bg-11-1627-2014>
- Zona, D., & Oechel, W. (2016a). FLUXNET2015 US-Atq Atqasuk. <https://doi.org/10.18140/FLX/1440067>
- Zona, D., & Oechel, W. (2016b). FLUXNET2015 US-Ivo Iivotuk. <https://doi.org/10.18140/FLX/1440073>